

## 2. Ebrach Bulk Storage Plant

The Ebrach bulk storage plant is located along both sides of a wide ravine out in the woods away from the village. The site has a paved highway passing the front and transversely across the ravine. An inconspicuous but large Administration Building together with a few small cottages are located by the highway at the entrance gate. Photograph No. 2, mounted below, shows a view across the ravine with the trunk highway and telephone lines in the background. The aforementioned photograph shows the destruction and scattering of 200 liter (52.8 gal.) fuel drums done by aerial bombardment. Photograph No. 3, mounted on the following page, shows the railroad spur following a contour of the ravine and the wooded hill on left in which the storage tanks are concealed. Photograph No. 4, mounted on the following page, is a view taken across the ravine from the aerial observation tower. There is an underground pump room entrance near the framed shed shown in Photograph No. 4. The Ebrach storage depot had all storage tanks located aboveground inclosed by masonry fragmentation protection walls and well camouflaged. All equipment such as pumps, foam generators, and CO<sub>2</sub> storage cylinders was installed in shallow underground rooms. A modern drum manufacturing and reconditioning plant was located at the upper end of the ravine. Allied bombing raids had done much damage to the railroad siding, drum storage yard, loading platforms, storage tanks and Administration Building. The drum manufacturing building and the underground equipment were undamaged.



PHOTO. 2  
EBRACH RAVINE  
NORTH of HIGHWAY



Photo 3  
Ebrach Ravine - Looking North



Photo 4  
Ebrach Ravine - Looking West from Observation Tower

The Ebrach storage depot originally had twelve 600,000 liter (158,500 gals.) benzene tanks and a few lube oil tanks. The earlier tanks were protected with brick fragmentation walls, whereas the tanks still under construction were being inclosed behind concrete walls 16 inches thick reinforced with six vertical 1/2 in. diameter plain, round rods located on 12 ft. centers around the periphery. The underground pump-house contained three 4-stage centrifugal pumps direct-connected to 17 Kw, 380 Volts "Y" connected, 1460 rpm, motors. The underground pump-room was undamaged but was very gassy due to benzene on the floor and due to the ventilation system being incapacitated.

There was evidence of "Jerry" can filling being done from railway cars by means of a 4-inch hose line running across the tracks above neighboring car couplers to the edge of the right-of-way and there terminating in an aluminum cap fitting having four 1 1/2 inch hose connections cast thereon.

Photograph No. 5, on page 7, shows a can filling machine. The machine is manually controlled and the cans must be lugged by hand. The main function of the machine was to proportion out the proper amounts of gasoline for filling ten cans at once. The ten compartments are filled by turning a control handle visible on the left end of the machine. This control handle opens a plug valve on the right end of the machine and the compartments are filled progressively by overflowing from one to the next until the last compartment is reached. At that time, the overflow passes out through a hose and is caught in a drum. A gauge glass on the left end of the machine indicates liquid level in the last compartment so little overflow occurs through the hose. For filling the cans, the machine has a "milker" arrangement whereby ten telescoping sleeves on the compartment outlets can be gang-dropped into the cans by throwing a lever. Then the bottom cocks on the "milkers" can be simultaneously opened by throwing another lever. Can handling onto a platform under the machine as well as off the platform must be done by hand. "Milker" nozzles are spaced 8 inches on centers whereas the "Jerry" cans are 6 1/2 inches wide. The supporting stanchions for the machine should have been spaced far enough apart for locating a roller conveyer underneath. The Photograph was taken of a machine which had been used as target practice at Ebrach; but the Americans had a complete machine at the Farge depot near Bremen.

Drum filling was done in an open shed. Photograph No. 6, mounted on the following page, shows a typical drum filling shed. Drums are filled on platform scales located flush with the floor. There are three scale dials visible in the photograph. Drums were rolled on the scales and filled by sliding drop sleeves from 1-inch "Autostop" valves. An "Autostop" valve was unscrewed and consigned to the Engineer Board, Ft. Belvoir, Virginia. The "Autostop" valve had a bell crank latch for holding the poppet valve open but there was no indication of the operating force which tripped the latch. From examination of badly sabotaged field equipment, it is thought that a "telegraph" wire was used for manual tripping when scale dials showed that a drum was filled. There was also evidence of drum filling stands located on concrete platforms by the railroad spur. This equipment had been inclosed by three-sided shelters.

The Ebrach bulk storage plant was built for the



PHOTO 5 - CAN FILLING MACHINE



PHOTO 6 - DRUM FILLING SHED

Wehrmacht and was quite thoroughly destroyed by bombing and sabotage. The drum manufacturing building with equipment could be used if deemed advisable.

(b) Underground Installations

1. Freiham Fuel Storage Depot

The Freiham Fuel Storage Depot is located about 10 Km. West of Munich and is served by a paved highway and railroad connection. The storage plant is said to occupy 500 to 800 acres in the pine woods overlaying a 60-foot deep gravel bed. The installation is under the direction of the "Wifo" organization which is apparently a semi-military German corporation devoted exclusively to the handling of liquid fuels for the "Wehrmacht" and "Luftwaffe".

The Plant was occupied at the time of the investigation by the U.S.A. 53rd QM Base Depot, Sub-Depot 5315, Captain C. M. Rusk, Commanding.

Drawing entitled, "Wifo Munchen", dated 9.7.45, bound herewith following this page, shows a plot plan of the tank installation, fuel lines, fire lines, pump houses, and railroad loading sidings. Tank numbers marked through with an "X" on the drawing have been damaged by bombing. Capacities of the Freiham storage tanks are as follows:

Tanks 1-32 incl., 872,850 gallons each except tank numbers 2, 3, 9, 10 and 18 which have been knocked out.

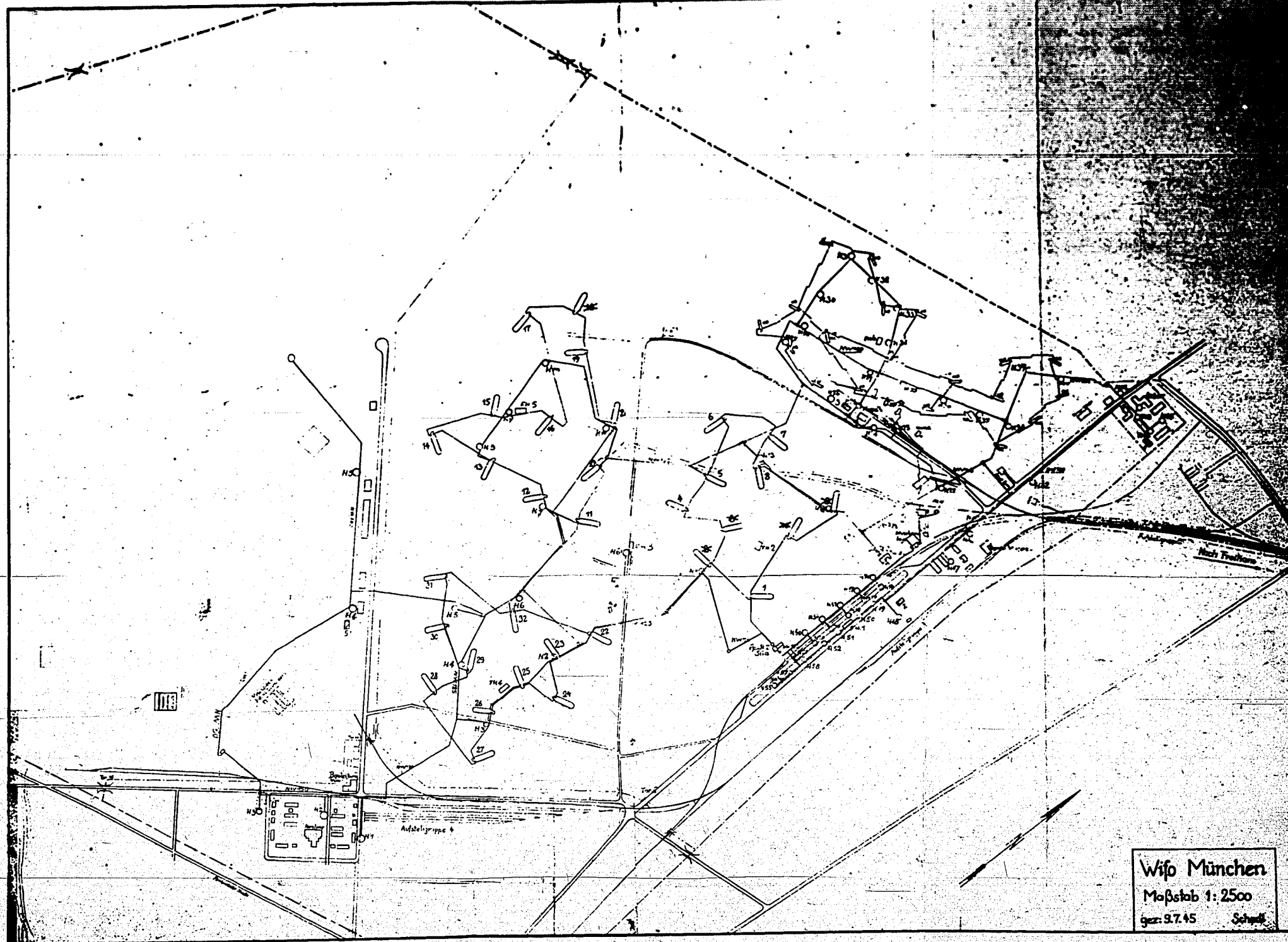
Tanks 101-120 incl., 79,350 gallons each except four tanks which have been knocked out.

Tanks 21-25 incl., 1,058,000 gallons each, under construction.

Tanks 31-35 incl., 1,058,000 gallons each, under construction.

It will be noted from the drawing that the present tanks are laid out in four groups and that the piping for each group forms a minor loop and the minor loops are in turn joined by piping into a major loop. Details of typical units comprising the installation are given in the following paragraphs.

The mixing installation consists of four working tanks of 300 cu. meters (79,400 gals.) capacity each. One tank of the group had been destroyed. There were four electrically-driven centrifugal pumps individually connected to the tanks. 10-inch diameter suction and discharge lines were used. Pumps were rated at 3,850 l./min. (1020 gpm) against a head of 30 meters (98.4 ft.). The direct-connected motors were rated at 31 Kw, 380-V. "Y" connected, 61-Amps., 50-cycle, weather-proof. There was a separate, small, vertical centrifugal pump with visibility for priming. Each tank was fitted with a pneumatic remotely-located liquid-level gage as well as a directly-mounted prismatic liquid level gage. The underground pump house is 50 ft. x 25 ft. and one side of it includes the ends of the four tanks.



Wifo München  
Maßstab 1:2500  
gez. 9.7.45      Schmidt

Photograph No. 7, below, shows the flat concrete entrance trap-door to the pump house. The gabled shed was built over the trap-door after reconnaissance planes had located them. Photograph No. 8, on the following page, shows the rear view of the shelter shed together with the rails for traverse movement of the heavy concrete slab. A slide covering the keyhole is discernible on Photograph 8. The Germans kept all rooms under lock and key and permission had to be obtained by telephone from the message center to enter any underground room. Photograph No. 9, on the following page, shows mushroom-type ventilator heads for a pumproom. Ventilating fans are mounted within the duct supporting the mushroom head. The pumphouse is ventilated by the aforementioned vertical blowers which draw 29 Amps. at 380 V.

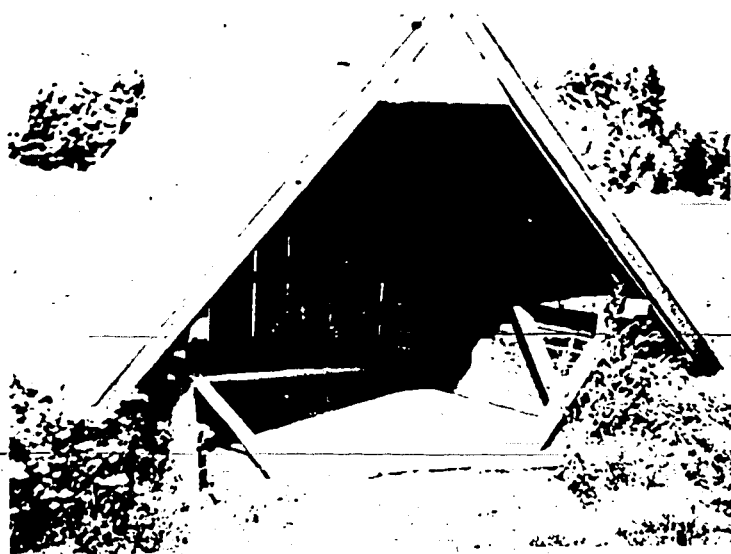
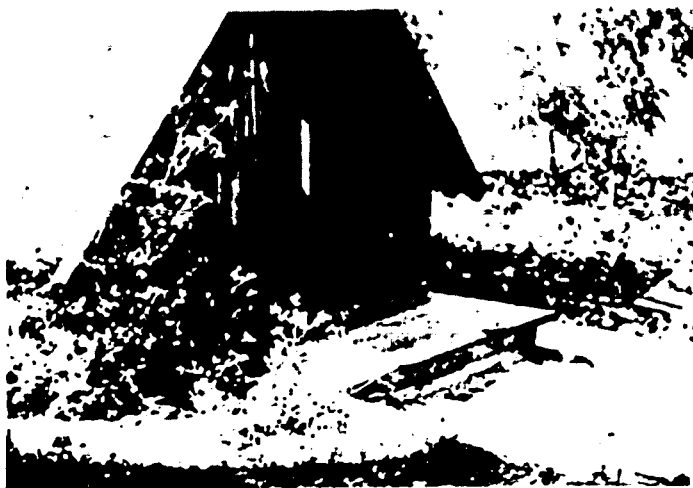


Photo 7  
*Shed over Entrance Trap-Door to Pump House*



*Photo 8  
Rear View of Entrance Shed*



*Photo 9  
Mushroom-Type Ventilator Heads*



The South pump station has the pump room floor 28 ft. 1 in. below grade. The pump room contains one main pump which draws from two 100 cu. meter (26,400 gals.) working tanks. The pump is of the same standard type and size as the transfer pump described in the following paragraph. In addition there is a one one inch vertical diffuser vane centrifugal pump with visi-gage for priming. The mixing pump could pump to the railroad siding or to the other storage tanks.

No. 8 tank installation has a pump pit at the end of the tank with floor level 32 ft. below grade. The tank is approximately 10 meters (32.8 ft.) in diameter by 46 meters (151 ft.) long and contains 3331 cu. meters (872,850 gals.). There is a rotary filter in an entrance room ahead of the pump pit. The pump room contains one 750 l./min. (198 gpm), 38 meter (125 ft.) head, 3-stage, 4-in. suction and discharge lines, pump. Pump is directly driven by a 9 Kw 380 V. motor. Pump room is ventilated by a blower which is controlled by a 15 Amp. switch. With this plan benzene must be double pumped in transferring from storage tanks to working tanks and finally to the railroad loading stems. Photograph No. 10, below, shows a 10 ft. diameter aperture made in a tank by a bomb. It will be noted that the tank shell was protected by a reinforced concrete armor wall. Photograph No. 11, on the following page, indicates the depth of the bomb crater which is estimated at 12 ft. Photograph No. 12, on the following page, shows a valve pit which was destroyed by a bomb.

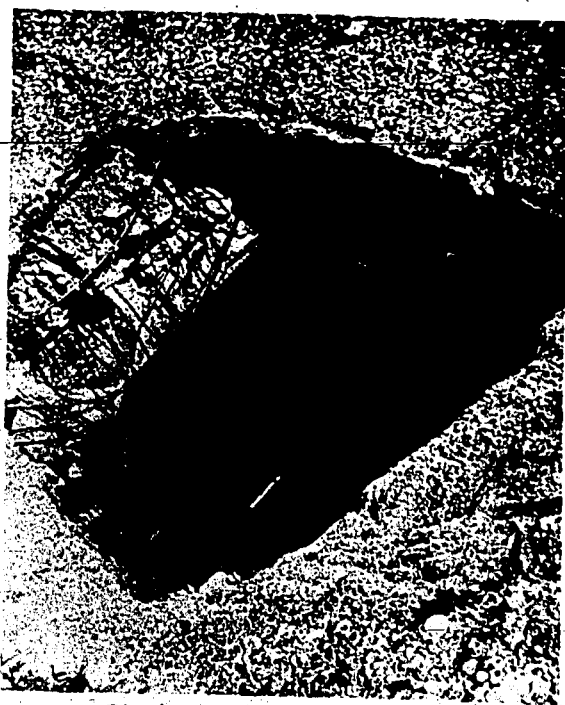


*Photo 10. Bomb Hit on Tank*



PHOTO. 11  
BOMB CRATER OVER TANK



PHOTO. 12  
VALVE PIT

Tank No. 108 installation is typical of the oil storage group which is located in the Northern part of the site. The tank has a capacity of 30 cu. meter (79,750 gals.) and has a pump room with floor 24 ft. below grade. The tank has a siamese connection on the end and is connected to a back geared positive displacement pump. The oil pump is rated at 7 cu. meters/hr. (31 gpm) and is driven by a 6 Kw, 220/380  $\Delta/Y$  Volt, 22/12.5 Amp., 1440 rpm motor.

The oil pump house was built at the end of a battery of six working tanks and its floor was 32 ft. below grade. Tanks were 7 ft. 7 in. in diameter and each had a capacity of 29.1 cu. meters (7690 gals.). Tanks were built in 1936. There were three pumps serving the six working tanks. Pumps were rated at 37 cu. meters/hr. (163 gpm) and were of the positive displacement toothed type. The pumps had six pipe connections. This type of pump was driven by a 23 Kw 220/380 Volt  $\Delta/Y$ , 1450 rpm motor. There was another type of rotary suction pump used for lighter oils. This pump was manufactured by Demag at Duisburg. This pump was rated at 113.5 cu. meters/hr. (500 gpm) when run at 2850 rpm. It was driven by a 13.5 Kw 380 Volt Y, 28 Amp., 2910 rpm motor. Signs designating products were painted on the ends of the tanks as follows:

Spülöl (rinse oil)	Gemisch (mixture)	Gemisch (mixture)
Sommermotoren Öl (summer motor oil)	Bottleöl (captured oil)	Wintermotoren Öl (winter motor oil)

A hot water circulating system is employed for heating oil storage tanks and transfer lines. The hot water circulating pump is rated at 340 l./min. (90 gpm) against a head of 33.3 meters (110 ft.) and is a 2-stage vertically split centrifugal pump with 3 in. pipe connections. Pump is driven by a 5.5 Kw 380 V.  $\Delta$ , 2880 rpm motor. Water is forced out at 100°C. and returns at 85 - 90°C.

The battery of five large tanks under construction had riveted plates 12 mm. (7/16 in.) thick and the tanks were not to be reinforced on the inside when completed. The tanks are 10 meters (32.8 ft.) in diameter by 52 meters (170 ft.) long, and have a capacity of 4000 cu. meters (1,058,000 gals.) including spherical heads. Tanks were to be lagged with steel wool covered with 3/16 in. welded wire reinforcing, plastered and incased in reinforced concrete. Thereafter the battery of tanks was to have been covered with 30 ft. of gravel for protection against bombing. Treatment of the inside of the tanks called for cleaning and coating with a layer of Portland cement 1 mm. thick and painting the cement with a benzene proof lacquer which was manufactured by the I.G. Farben industry. Photograph No. 13, on the following page, shows a battery of 1,058,000 gallons tanks. Photograph No. 14, on the following page, shows a 1,058,000 gallon tank with camouflaged netting. Photograph No. 15, mounted on page 15, shows the base and supports for the 1,058,000 gallon tanks.

There is a diesel engine driven emergency power plant



*Photo 13. Battery of Million Gallon Tanks*



*Photo 14. Million Gallon Tank*

installed as standby to the high line electric service. Power house is built under a fill equivalent to a grade separation and has an easy downgrade ramp entrance. A nameplate shows that construction took place in 1935. The diesel engine was manufactured by M A N and is rated at 590 hp at 428 rpm. The diesel engine was equipped with an exhaust gas driven turbo supercharger manufactured by Brown-Boveri in 1935. Supercharger ran at 18,600 rpm and delivered 480 cu. meters/min. (17,000 cfm).

Photograph No. 16, on the following page, shows a quick coupler for portable pipe. Quick couplings of the toggle lever type have doughnut shaped rubber ring gaskets 9/16 in. in cross sectional diameter for 80 mm. (3.15 in.) pipe and 3/4 in. for 100 mm. (3.94 in.) pipe. This type of pipe was used in several parts of the storage depot where the permanent piping had been bombed out.

Photograph No. 17, on the following page, shows a standard loading stem for tank cars. Vertical riser is of 5 in. pipe and the hose is a 4 in. I.D. heavy wire wrapped synthetic rubber hose with aluminum couplers.

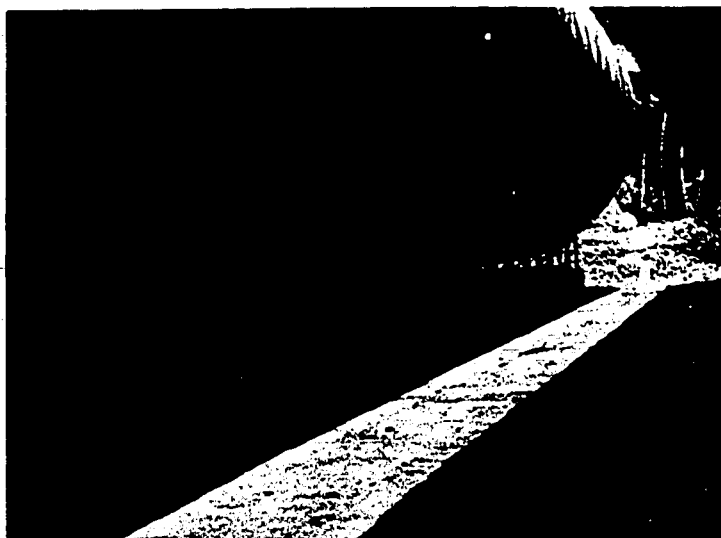
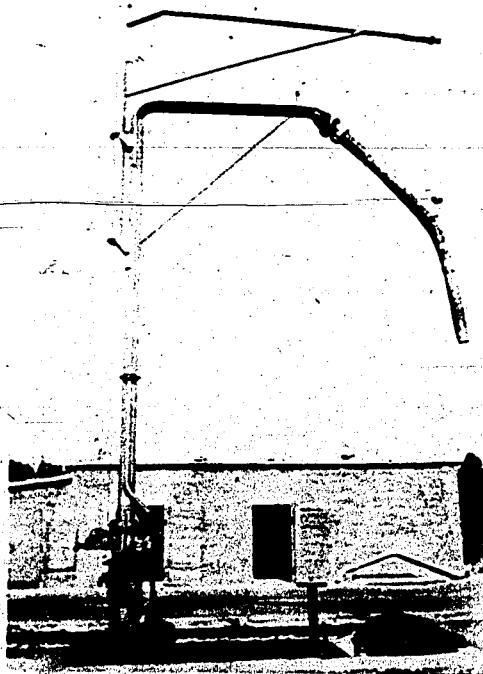


*Photo 15. Base for Million Gallon Tank*

Photo. 16  
QUICK COUPLER-PORTABLE  
PIPE



PHOTO. 17  
TANK CAR LOADING STEM



## 2. Nienburg "Wifo" Bulk Storage Depot, Nienburg

The Nienburg "Tank Anlage" is a storage and blending plant for liquid fuels and lube oils. The grades of fuels and oils handled are benzenes and lube oils, hence, the plant is divided into two separate groups on that basis.

Fuels and lube oils are brought into the plant in tank cars on a railroad siding which runs along the southeast side of highway No. 215 leading from Minden to Nienburg. The Weser River bounds the northwest side of the property, and dock facilities have been built on its right bank.

There are five connections for unloading tank cars of lube oil at the railroad siding. A connection consists merely of a valve placed horizontally aboveground with a wire wrapped 4-inch hose remaining connected thereto. There are 30 vertical overhead tank car fill stems with wire wrapped 4-inch hoses and Wilke "Gasometers" connected thereto. The "Gasometers" consist of an aluminum casting with float arrangement for shutting off flow of fuel when cars are full. The "Gasometer" cover replaces tank dome cover when car is being filled. There was also a 4-in. valve and hose connection for bottom unloading of tank cars of benzene in each valve pit by the tank car fill stems. A track scale is provided for weighing tank cars. Track over the scale is fixed stationary and the scale is loaded by an electrically-operated elevating plate which raises the car off the rails by taking the load on the bottom of the wheel flanges.

A drum cleaning shed is provided in which drums are cleaned with rinse oil and steam. Horizontal rollers rotate the drums after rinse oil and a chain have been placed inside. Next the drums are rotated on an axis adjustable with the vertical for cleaning the ends of the drums. After that the drums are rolled to a stand over a pit where oil is drained out and the drum is subsequently steamed. Drain oil and condensate is pumped from the pit and reclaimed by centrifuging. All handling of drums is by manual rolling.

Oil drums are filled with automatic stop valves and weighed on platform scales having large dials.

A mixing pump house for oils had been blasted by the "Wifo" organization upon orders from the German Wehrmacht. Mixing pump house and storage consisted of four small tanks, about 100 cu. meters (26,400 gals.) capacity each, and two circulating pumps. Oils were pumped to this mixing station from the oil storage tanks and blended by circulation.

A separate drum filling shed provided for benzene. Benzene Drums are filled on platform scales and flow is controlled by hand-operated cocks.

An underground boiler room with floor 21 ft. 1 1/2 in. below grade is intact. It contains two scotch marine type boilers and feed water treating equipment. Boilers operate at 10 Atm (147 psi) pressure.

The whole installation is electrically powered at 380 V. but a standby diesel engine driven generator is provided. Generator is a 500 KVA 400 V. machine direct-connected to a six-

cylinder 1: A 1" diesel engine, Pse (horsepower) 590 rpm 428. The engine is equipped with an exhaust gas driven turbo supercharger built in 1935. Engine room is built at grade but is mounded over for protection.

There are three groups of oil tanks each having nine tanks in a minor loop and all groups are joined into a major loop with pipe. Oil tanks have steam coils for heating and oil lines have steam tracer lines. Tanks hold 360 cu. meters (95,000 gals.) each and are provided with an underground pump pit. Pump pit floor is 24 ft. below grade. Pump motors are 6 Kw, 1450 rpm, and are back-gearred to rotary pumps delivering 6-7 cu. meters/hr. (26-31 gpm). Pump pit has one "total" C7 CO2 fire extinguisher.

There is a benzene storage and transfer installation not far from the railroad siding and also not far from the former tetraethyl lead blending plant. It consists of two 100 cu. meter (26,400 gals.) tanks and a pump pit with floor 27 ft. 4 in. below grade. Pump is a single-stage centrifugal type and delivers 180-200 cu. meters/hr. (790-880 gpm). There are four 30 Kg CO2 cylinders in a cell adjacent to the pump room. Operation of the CO2 system is by means of a pull cable with handle near the entrance door.

The tetraethyl lead blending plant has been blasted by the "Wifo" organization. The benzene tanks are arranged in three groups of ten tanks each. Seven of the tanks have been knocked out by bombs. Each group of tanks is loop-connected by a pipeline and the groups are connected into a major loop. Each benzene tank has a capacity of 3320 cu. meters (876,000 gals.) and has an individual pump pit. Pump pit floors are 42 ft. below grade. Pump is rated at 100 cu. meters/hr. (440 gpm) and is directly driven by a 22 Kw motor.

A booster pump room is installed on the pipeline from the river for unloading barges. Pump room contains one 100 cu. meter/hr. (440 gpm) centrifugal pump driven by a 22 Kw motor. There are ten 30 Kg CO2 cylinders in a room adjacent to the pump room for fire protection. Operation is by means of a trip cable with handle located near the grade entrance. There is an 8 in. oil line and a 3 in. vapor line leading down to the dock to a pump set formerly located on a floating dock. This pump set had been blown up by the "Wifo" organization. Fire protection for the plant as a whole is provided by a loop of 6-in. high pressure underground water lines around the whole site. Hydrants are located at frequent intervals in the woods and all are plainly marked for location by having several sign boards pointing toward them giving distances in meters to the hydrants. A fire shed was located among each group of tanks and contains a trailer complete with "Tutogen" foam equipment and two hoses for hydrant connections. In addition there is one large fire truck with "Tutogen" foam apparatus. The portable fire truck had been run into the city of Nienburg for safe keeping. Benzene pump rooms had quick fire protection by a battery of CO2 cylinders; and the heavy oil pump rooms by portable foam extinguishers.

One benzene tank of the seven which were hit caught fire. Another tank had four bomb hits in a row along the top center line. Another tank had been punctured by a single bomb hit but this tank had only 6 ft. of earth cover over a layer of 26 in. of reinforced concrete.



with 7/8 in. diameter bars on 18 in. centers both ways. The tanks which were ruptured were reinforced with heavy angle iron trusses on 6 ft. centers through their full lengths.

### 3. Farge Fuel Storage Depot, Farge

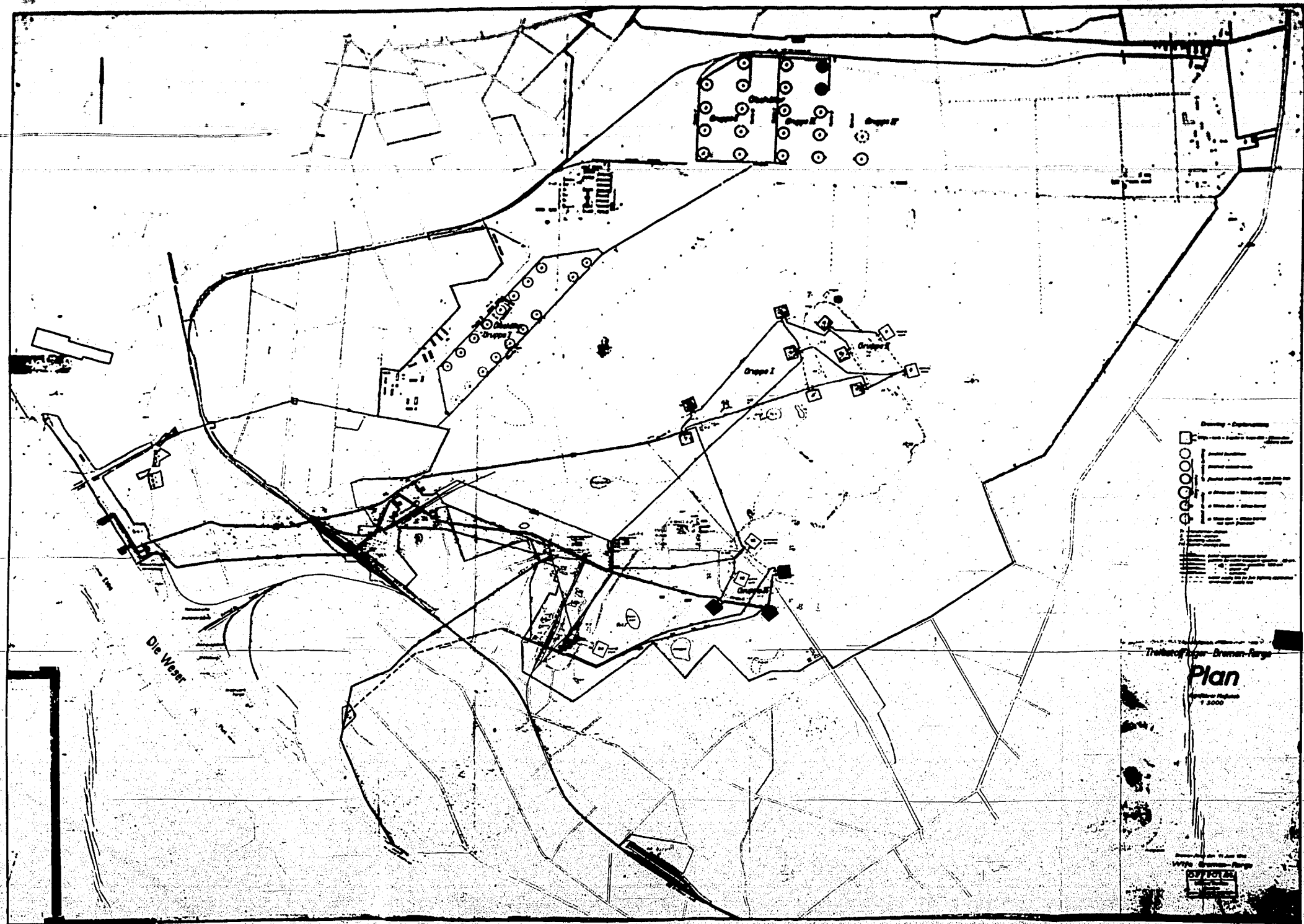
The Farge Fuel Storage Depot is located inland about one mile from the village of Farge, a northern suburb of Bremen. Fuel can be transported into the depot by ocean transports, river barges, or railway tank "wagons". Drawing No. A1/1, entitled "Wifo Bremen-Farge", shows a plot plan of the depot. There are three docks and two railroad yards for loading or unloading liquid fuels.

The storage plant consists of 15 blocks of five tanks each. Each block has a capacity of 126,000 Bbls. (5,290,000 Gals.) Total storage capacity is 1,890,000 Bbls. (79,400,000 Gals.). Storage capacity was far beyond German production capacity because it was reported impossible to ever fill more than two or three blocks after the French invasion. The Depot was planned for the storage of benzene, kerosene, and diesel oil, and was enlarged to include lube oil storage.

Tank storage is dispersed with blocks, 1-10 inclusive, in one area and, blocks 11-15 inclusive, in another area. Blocks are connected with a loop oil pipe line and by underground fire lines. The Depot was built in 1939 at a cost of 80,000,000 Reichsmarks.

Ship Docks are "T"-shaped steel structures in plan view with a walk and pipe gallery approach well above high tide. Dolphins are formed of four box-shaped steel piles braced together. An 18-inch fuel line and a 12-inch fuel line on each side of the walk lead from the dock manifold back to the temporary pump shed on piling at the shore line. In addition, a 6-inch vapor line, a water line, and a steam line are carried along one side of the walk. Vapor return line is not used for that purpose. The temporary booster pumphouse contains three centrifugal pumps having 65 Kw. 380 V., 1465 RPM motors direct-connected to two-stage centrifugal pumps having a rated capacity of 160 m.<sup>3</sup>/hr. (704 gpm) against a head of 40 meters (131 ft.). The water line along the dock was the only visible fire protection for that area.

The four oil lines run up the river bank a short distance to an underground surge tank room. This building contains three large gasoline filters, four diesel oil filters, explosion arrester, together with four 50 m.<sup>3</sup> (13,200 Gal.) tanks. These tanks have a working pressure of 10 Atm (147 psi) and have safety valves set at that pressure to pop to the outside. The tanks are carried full of compressed air for leveling out the impulses of the ship's direct-acting steam pumps. The filters are large circular pressure vessels with four 12-inch multiple basket filters therein. The explosion arrester is a 1600 l. (422 Gal.) pressure vessel with bronze screens inside and is rated at 10 Atm (147 psi) working pressure. Differential gauges are installed around the filters. Pressure gauges, recording orifice type flowmeters, and indicating liquid level gauges are installed in the underground control room adjacent to the ends of the tanks. Fire protection for the tank room consists of a bank of thirty-two 30 Kg. CO<sub>2</sub> cylinders located in a separate cell and having a manually-operated trip cable for flooding the room. The manual CO<sub>2</sub>



release also shuts off all electrical power in the underground workings. The tank building also contains a transformer for drying motor stator windings at reduced voltage. Drying transformer is rated 380 V. 130 V., 1 KVA, 45.3 Amperes. This system of drying motor windings is used throughout the depot.

The liquid fuels are forced from the surge tanks to the separate blocks of storage tanks. There are five 4,000 m.<sup>3</sup> (5,280,000 Gals.). The tanks are coated on the inside with 1-2 mm. of portland cement and painted with "Lithurin", a product of I. O. Farben. The storage tanks are horizontally constructed, rivetted tanks with hemispherical ends and are protected with one meter (3.28 ft.) of reinforced concrete and six meters (19.68 ft.) of earth over their tops. With the above protective cover, only one tank was lost in an air raid during which 1500 bombs were dropped. The loss of the one tank was attributed to a second 1000 lb. bomb landing in a crater made by a previous bomb. An inspection manhole and gauging gallery of reinforced concrete is built along the top center line of the tanks. A 4-inch vapor line with manually-operated release cock is installed in the inspection gallery. Vapor pressure is released from the tank before gauging.

Pump rooms for the battery of tanks are located with their floors 38 ft. 8 in. below grade. There are three pump rooms across the end of the battery. Two tank heads project into each of the two outside pump rooms and one tank head projects into the center pump room. Each tank has an individual pump and all pumps are manifolded together. The pumps are three-stage, 5,000 l./Min. (1320 gpm), 12 Atm (406 ft.) head, 1470 rpm centrifugal pumps direct-connected to 130 KW 3,000 Volt motors. A piping gallery and filter are located above the pump room on a mezzanine floor built of steel grating. A "Hannemann" regulator which prevents over filling of tanks, is located on the upper level. Piping is connected to each tank through two manheads in the end. One manhead is located on the diametral center and the other in the lower quarter of the head. Liquid can be recirculated and mixed in a tank by pumping because the fill line extends far into the tank and has an eductor nozzle on the end. The pump room has an instrument board with all necessary instruments for each tank and pump. Instruments include liquid level gauges, pump pressure gauges, differential gauges for the filter, recording flowmeters, and indicating flowmeters. Pump room is ventilated by a single motor located on the lower floor. This motor has an induced ventilating blower coupled on one end, and a forced ventilating blower coupled on the opposite end.

Fire protection for the underground rooms is provided by CO<sub>2</sub> flooding and by portable hand-operated foam extinguishers hanging on the walls. There are twelve 30 kg. (66 lb.) CO<sub>2</sub> cylinders for the upper level rooms and twenty-four CO<sub>2</sub> cylinders for the lower level. Release of the CO<sub>2</sub> is by means of a pull cable with handle located under glass near the door. The portable foam extinguishers are the "Total C-7" make and size.

The mixing block consists of one group of large tanks, 4,000 m.<sup>3</sup> (1,056,000 Gals.) capacity each, 10 m. (32.8 ft.).

diameter by 56 m. (164 ft.) long overall. A 300 m.<sup>3</sup>/hr. (1320 gpm) pump is installed for each tank. Each pump is driven by a direct-connected 130 KW 3000 volt motor. There are four main lines 250 mm. (9.84 in.) diameter across the pump room. These lines allow great flexibility in choice of mixing, either in one tank or between tanks. In one case, two valves are operated by one handwheel and shaft by extending the shaft through the driving pinion. One of the valves is closed while the other is open. Pump room is fully equipped with gauges mounted on a central panel board. Gauges include liquid level, pressure, vacuum, differential, and recording flowmeter. Pump room is ventilated by a 13 KW motor having an induced blower coupled to one end of the shaft and a forced blower coupled to the opposite end. Fire protection consists of a bank of CO<sub>2</sub> cylinders and portable foam extinguishers as described in foregoing paragraph covering a battery of storage tanks.

The shipping pump room located near the railroad, consists of eight 100 m.<sup>3</sup> (26,400 gals.) tanks and four pumps. Pump room floor is 31 ft. below grade. Pumps have a capacity of 5,000 l./min. (1320 gpm) against a head of 110 m. (361 ft.). Pumps are direct-connected to 145 KW, 3,000 V., 1470 rpm motors. Ventilation is forced and induced from fans in the basement. Fire protection consists of a bank of fifty 30 Kg. (66 lb.) CO<sub>2</sub> cylinders and portable "Total C-6" extinguishers.

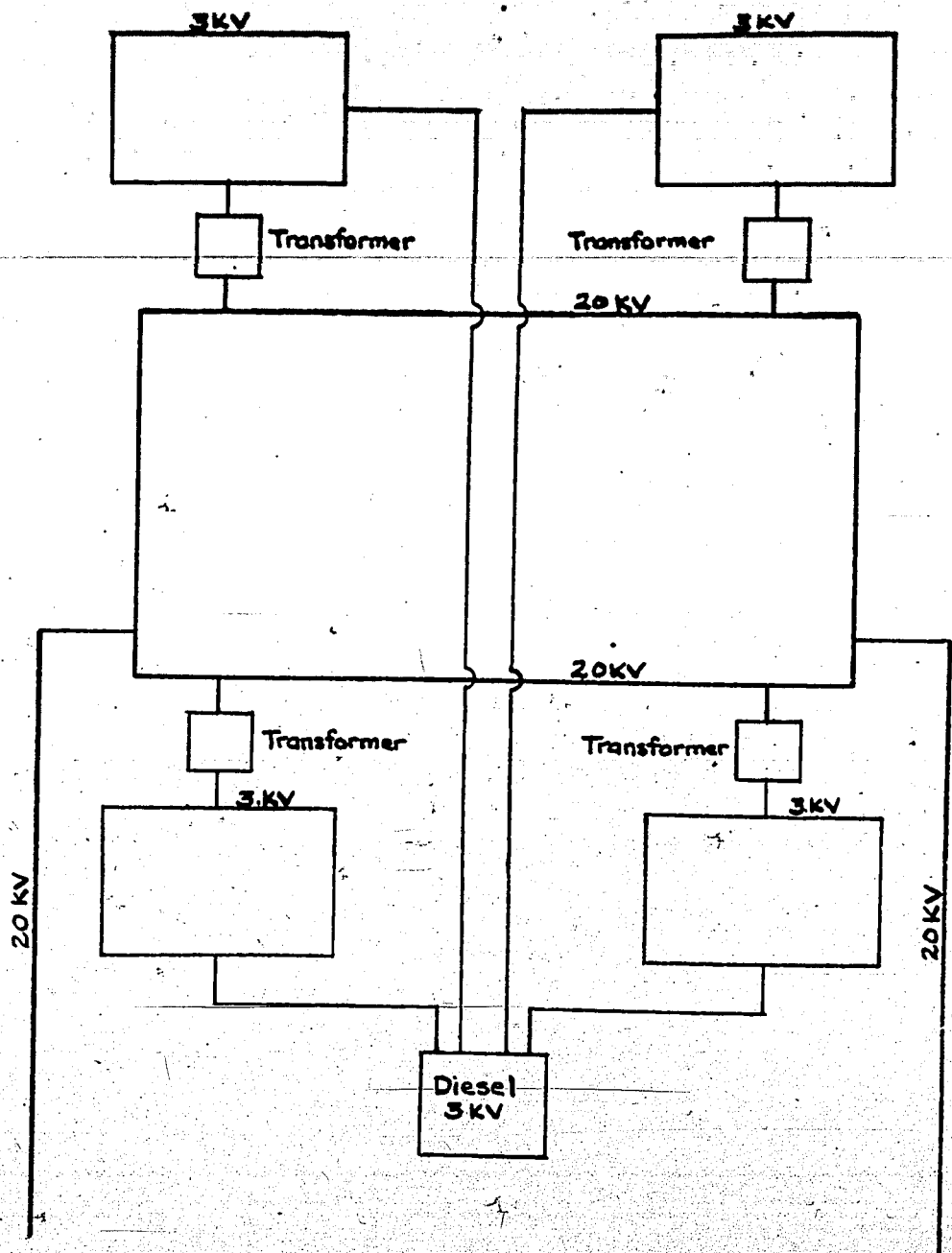
Power for the depot is distributed through transformers located in a room with floor level 13 ft. below grade. Sketch No. 1 herewith shows potentials of power distribution loops.

There is a telephone and signal system which ties in every basement entrance with the message center. An operator must telephone the message center before entering an underground room. There is a door-operated switch which flashes a light on a board in the message center whenever entry is made.

## 6. RECOMMENDATIONS

(a) The storage of liquid fuels in aboveground tanks protected by masonry walls at Ebenhausen and Ebrach did not prove successful for the Germans. Tanks were bombed from the air, loading points at railroad sidings were hit and visible buildings were destroyed from the air. The underground pump rooms, foam control rooms, and boiler houses at these same depots were not damaged, although they were vulnerable to attack due to the shallow cover of earth over them. The advantage of underground installations lies in the overgrowth of vegetation and trees which obscure their definite location from the air. There were no visible indications that the masonry fragmentation walls had contributed anything toward saving tanks. The efficacy of masonry walls for preventing damage to tanks is questioned. There was evidence that tanks inclosed by masonry walls were easily and freely sabotaged.

The wide use of aluminum for hose couplings, terminal fittings, float controls, pipes and tanks might well be emulated in the U.S.A.



ELECTRICAL DISTRIBUTION SYSTEM  
FARGE FUEL DEPOT

SKETCH NO.1

26

(b) The fuel depots at Preiham, Nienburg and Farge are, among others, good examples of underground fuel depots which successfully withstood "pin point" aerial bombardment with small losses. The elaborate underground installations were made possible by an economy geared primarily to war.

It is considered that the fuel depot at Farge establishes some good principles of construction. The 1,000,000-gallon steel tanks are protected by a layer of reinforced concrete up to 1 m. (3.28 ft.) thick. In addition, the tanks are mounded over with about 9 m. (29.52 ft.) of gravel including a layer of top soil. The theory behind this construction is that the gravel will withstand the bomb burst and dissipate resonant concussions; and the reinforced concrete layer will act as armor as well as provide a load carrying arch. It was planned to fill in bomb craters by using earth moving machinery immediately after an attack.

The forced ventilation system enabled the Germans to operate their underground caverns without danger from explosions.

The use of extensive cross connections of piping, commonly found on the Continent, is considered superfluous.

The resistance of underground fuel storage depots to attack show conclusively that permanent bases warrant the storage of liquid fuels in that manner.

FILE NO.  
B.I.G.S. - 112

COPY NO. 1  
16 October 1946

This Interrogation Report contains Information from a German  
Scientist exploited by United Kingdom.

COAL AS FUEL FOR THE REGENERATOR  
GAS - TURBINE

by

L. RITZ  
J. KARWEIL  
P. HENTRICH

LIBRARY  
of the  
FOREIGN SYNTHETIC  
LIQUID FUELS DIVISION  
Bureau of Mines

DEC 17 1946

WARNING: Some products and processes described in this report may be the  
subject of U.S. patents. Accordingly, this publication cannot  
be held to give any protection against action for infringement.

JOINT INTELLIGENCE OBJECTIVES AGENCY  
WASHINGTON, D. C.

Reports and Translations No. 78.  
Date : June 1<sup>st</sup>, 1946.

UNCLASSIFIED

( M.A.P. VOLKENRODE ) *omit*

... COAL AS FUEL FOR THE REGENERATOR-GAS-TURBINE.

BY

L. RITZ,

J. KARWEIL, AND P. HENTRICH.

M.A.P. Völkenrode Ref: MAP - VG 9 - 78 T

13



### COAL AS FUEL FOR THE REGENERATOR-GAS-TURBINE.

Only when coal is used as fuel, the gas-turbine is in several fields competitive with the hitherto applied power engines. Various possibilities, resulting from the working conditions which exist particularly at this power-plant have been investigated in detail in order to guarantee a possibly large working field for the RGT. The present paper gives a summary of the results obtained until now and points out two possibilities which seem to be particularly promising and which shall be discussed more thoroughly in special reports. Moreover these reports may have more general validity with regard to the use of coal in gas-turbine engines, boiler firings, and jet nozzles.

#### Summary

##### A. Direct combustion of

- 1.) Flow coal
- 2.) Coal in lumps
- 3.) Fine coal

##### B. Coal vaporization with

- 1.)  $\text{CO}_2$  - addition
- 2.)  $\text{H}_2\text{O}$  - addition

#### A 1 Direct Combustion of Flow-Coal.

With the direct combustion of coal, we may utilize the experience obtained with oil combustion chambers by adding finely ground coal to the fuel oil. Such oil-coal-suspensions are wellknown under the name of "Flow-coal". Until now the use of this flow coal has always failed on account of the separation of the coal, when storing, in form of a viscous sediment, which cannot be stirred any more. Numerous experiments failed which were undertaken to prevent this effect by adding chemical media which were meant to act as stabilizers. Only recently the application of physical methods, with different kinds of coal and oil, has yielded suspensions which did not show any sediment even after storing for several months. By means of

these methods we are able to produce a flow coal, which can be pumped, with a proportion of coal up to a weight-percentage of 35. There is no essential difference between the combustion behaviour of pure<sup>st</sup> and of flow coal. Using prepared coal, the proportion of ashes, according to demand, may be reduced to below 0.5 p.c.

#### A 2 Direct Combustion of Coal in Lumps.

When using coal in form of lumps the admissible load of the combustion chamber in the present state of technics decreases by nearly two powers-of-ten as against the combustion chambers for liquid fuel. With coal firing we generally calculate with  $0.25 \times 10^6$  cal/m<sup>3</sup>h, whereas in the combustion chambers of gas turbines  $40 - 60 \times 10^6$  cal/m<sup>3</sup>h are attained. It is true that with locomotive boilers with coal powder firing  $1.5 \times 10^6$  cal/m<sup>3</sup>h were obtained; but this is a very small amount compared with the combustion chamber of the gas-turbine and was possible only when renouncing a complete combustion and, moreover, only for a short time on account of the high deposition of ashes causing the formation of "swallow nests". By changing to coal firing one of the main advantages of the gas-turbine plant viz. the small space required, is reduced considerably. What renders the problem more difficult is the fact that, due to the peculiarity of the processes, pressures up to 20 atm occur in the combustion chamber of the gas-turbine. The advantage aspired with the change to coal firing, namely the reduction of the running costs, decreases or becomes doubtful owing to the amortization of the increased production costs of the large pressure-proof combustion chambers.

Thus the performance of coal combustion chamber must be increased appreciably in order to make the use of coal for turbines promising. As is well known, the combustion process on the surface of the coal can be intensified extremely by an increase of the supply of oxygen: this is possible on principle by increasing the pressure and the velocity of the combustion air.

The pressure of the combustion air is generally given by the gas-turbine process, and with the open process is sometimes less than 3 atm (abs) with moderate turbine-entry temperature and with high grade utilization of the exhaust heat; this pressure rises with increasing turbine-entry temperature,

furthermore with introduction of recombustion and with a restriction of exhaust heat utilization caused by the construction, and finally attains values of more than 20 atm when applying the semi-open gas-turbine method proposed by S u l s e r.

Thus we may dispose only of the velocity of the combustion air for increasing the load of the combustion chamber. The experiments of P r e d w o d i t e l j e w, Z u c k a n o w a, Z u c k a n o w, and G r o d z o v s k y have shown that the intensification of the substance exchange and with this the combustion velocity can be increased considerably by a turbulent incoming flow. The only supposition is a sufficiently high temperature in consequence of which the chemical reaction velocity is so high that only the physical exchange of substance is decisive for the combustion velocity. This fact is secured with temperatures of more than 800° C. On account of the high velocities of flow the small lumps of coal must be fixed somehow in order to prevent that they are torn away with the combustion air.

In case of firing lumps of coal the coal is fixed by gravity, this is sufficient with the slight velocity of flow ( $< 5$  m/s). In the same measure as the coal burns up the particles become smaller but with the usual method of firing the coarse lumps of coal are added from above, so that even smallest particles can be taken away unburned in relatively small quantities only. The chiefly used coal sticks and frits besides; thus the coal becomes coherent by itself.

With the powder firing, too, we find similar conditions. Gravity and friction force act against one another thus effecting a relative velocity between gas and particles, necessary for the substance exchange, i.e. for the combustion. In the usual firing the maximum relative velocity is equal to the hovering velocity. By this a certain shortest combustion time is fixed for every magnitude of the particles. The air velocity can be increased to any degree but the relative velocity and, with this, the combustion velocity will not be raised at the same time.

If we want to utilize the high flow velocities occurring in the gas-turbine process for intensifying the inflow and, with it, for shortening the combustion time, the coal must be fixed either by special guide forces (double-grates) or by mass forces (centrifugal force).

Guide forces have already been used experimentally for the boiler firing, keeping the coal down by incombustible bodies. But this arrangement implies a high resistance of flow and is thus rather disadvantageous. Performances of  $50$  to  $100 \times 10^6$  cal/m<sup>3</sup>h with flow velocities of  $30$  m/s resulted from tests with a modified double-grate of metal sheets  $1$  mm to  $10$  mm thick, arranged circularly at a distance of  $3$  mm and flown through in longitudinal direction, the coal - anthracite - or "Esskohle"\*) respectively, being in the interior of the cavity between the grate metal sheets.

Such a combustion chamber would thus be absolutely useful. Technically it would be designed in form of a series of long narrow bags arranged abreast. The burning out, however, is very unsatisfactory. In consequence of the thermal stress the larger coal lumps burst and the particles smaller than the grate width are taken away. These particles can of course be separated in a "Zyklon" arranged behind the combustion chamber. Such a combustion chamber is not perfect in respect of operation for other reasons, too, since it is difficult to prevent the ashes from melting and sticking to the grate rods. During the tests the melting and sticking to the rods was not observed but we must consider the fact that in the case of application the temperatures are considerably higher. Finally the problems of the supply of coal and the removal of ashes must be solved. The application of sticking coal will presumably render the replenishment difficult. Gas-coke may be used and keeps burning even when blown with cold air. Previously smouldered coal was likewise used with excellent result.

Another method to fix the coal by means of guide forces is that of using briquettes. They are either supplied in form of thin plates by means of rails and burned up in longitudinal direction, or, in form of bodies of square or circular cross section or perhaps as an infinite line, are led through a suitably shaped duct towards a nozzle, from whose opening a violent jet of air blows against the frontal area of the line. The line is advanced in the same proportion as the frontal area burns up. Both these methods have been investigated; at flow velocities of  $30$  m/s the results were the following: When using plates we obtain  $100 \times 10^6$  cal/m<sup>3</sup>h, using the line  $20 \times 10^6$  cal/m<sup>3</sup>h. The volume of the coal outside the combustion

\*) of  $10$  to  $20$  mm in diameter

chamber was not considered in this calculation. The tests have shown that numerous fine rents in the briquettes result from the thermal stress; on account of the missing heat radiation a temperature occurs in these rents which is higher than that on the surface; the combustion in the rents, therefore, is quicker. Consequently the rents become wider, especially on the ground. Thus a deeply articulated surface results which consists of numerous coal heads with reduced basis-cross section. These heads are easily broken off and taken out by the airstream. The volume of the single particles thrust out was up to  $2$  cm<sup>3</sup>. The losses caused by this insufficient burning out amounted approximately up to  $50$  p.c.; they are too high for practical use.

Also the sort of coal is of certain influence on this phenomenon. Grained and briquetted gas-coke did not show any losses of flight. The plates were very firm and, at the ignition were covered with an adhering brownish layer of ashes; when blown with cold air, these plates did not continue burning. With regard to the losses of flight no differences could be noted, using either anthracite, "Esskohle", or "Gasflammkohle". Such a difference existed in the combustion behaviour only. When more gas is contained in the coal, the coal burns more quickly. "Esskohle" with a contents of ashes of  $0.7$  and of  $10$  p.c. has not shown any difference with regard to ignition, combustion behaviour, and flight losses. The smallest losses occurred with smouldered briquettes.

Sulphite-waste liquor and pitch were used as a bond. Pitch has the disagreeable property of becoming soft when heated: pitch-briquettes, therefore, are of little mechanical solidity. When smouldering, however, the application of pitch is suitable, particularly with non-sticking coal because the pitch cokes with smouldering temperature and cements the single coal particles.

As already mentioned above, it is possible to fix the coal by centrifugal forces. Putting coal into the interior of a rotating ring, a fastly adhering coal ring will form with sufficient turning speed; this coal ring can be blown through axially or radially. Strictly speaking, we have to deal with a combination of guide and mass forces, since one part of the double-grate has been substituted by the centrifugal forces.

Without experiments we cannot determine whether or not this method means a special advantage as compared with the double-grate. There still is one half of the grate at which the ashes can melt and stick, and through which unburned particles can be taken out. When applying the centrifugal ring, we have the possibility of slinging the ashes off in liquid form but we have to overcome the difficulties resulting from the construction of such a heavily loaded glowing body. This mechanism cannot be enlarged unlimitedly since the effect obtained increases with the square, and the space required increases with the cube of the apparatus dimensions.

Summarily we may make the following statement: The hitherto investigated combustion chambers for lumps of coal - they be "Nusskohle" or briquettes - have the disadvantage of causing important losses of flight, and difficulties in preventing the melting and sticking of the ashes at the guides. During the tests, cold air was used for blowing; high temperatures at the guide mechanism, therefore, did not occur. The process of melting and sticking at the guides was observed only when working with the efficient combustion chamber for coal-plates. It is possible, of course, to proceed from highly disashed coal and to separate or to burn the flight losses in a "Zyklon" arranged behind; detailed investigations, however, will be necessary.

We must now make the following demands from a coal combustion chamber:

- 1) Since coal falls into pieces by thermic strain the chamber must consume even most finely ground coal without losses of flight.
- 2) In order to prevent the melting and sticking of ashes at the guides, the interior of the combustion chamber must be designed without installations.

### A 3 Direct Combustion of Fine Coal.

The above demands necessarily lead to powder firing. At the beginning of this paper we have already stated that in this case it is not easily possible to increase the effect of the combustion chamber. The particles cannot be blown against turbulently - only by this method the above mentioned results were obtained - because a relative velocity, much higher than the velocity of sound, would be necessary to blow against a

particle of  $10\mu$  at  $1000^\circ\text{C}$  turbulently. But even in the laminar range an increase of the relative velocity can be obtained by the application of centrifugal force, which shortens the combustion time. The fixing of the particles in the chamber by something like a sieve, until they are burned up entirely or partly, gives a progress in the desired direction. This progress can be obtained by performing the combustion in a sifter. Here the coal burns within a vortex flowing inward from outside. The centrifugal force acts against the flow direction so that relative velocities can be attained exceeding the hovering velocity by far. The particles can be taken out of the chamber by the airstream only when they are burned to such a size that the friction force is greater than the centrifugal force. By appropriate dimensioning of the guide system and of the chamber diameter, we are able to adjust the desired sifting effect. This effect is intensified by the increase of the specific weight of the particles while burning out.

Without special tests we cannot decide whether the sifter combustion chamber must be designed with or without a system of guides. The chamber without this system permits a simple supply of coal. In this case, however, we must consider the fact that particles are rubbing at the exterior wall, fall down to the ground, and remain there or circulate slowly. This will cause an accumulation of unburnt coal in the chamber, which would disturb the vortex considerably. This cannot occur in a chamber with a system of guides, but in this case the supply of coal is more complicated.

By a suitable construction we are able to separate one part of the ashes in solid or, when using high temperature, even liquid form. The question whether or not the gas needs recleansing depends on the erosive behaviour of the ashes.

The coal grain, on an average, must be smaller than  $0.5\text{ mm}$ . Preliminary tests have shown that coarser grains fall down quickly. Partly they remain there and partly they rotate slowly with the vortex and do not continue burning. The height of the chamber must be made so great that the grains meet the ground only when burnt to ashes.

It cannot be determined beforehand whether the total quantity of air or only part of it must be sent through the combustion chamber. When the whole quantity of air is passed we may perhaps obtain a nearly uniform distribution of temperature over the cross section and thus may spare the additional space for a mixing chamber; we have, however, to consider the fact that by the temperature drop thus caused, the combustion time will possibly be decreased too much.

An advantage of the sifter combustion chamber, as compared with the combustion chamber for lumps of coal, is the simple mastering of the regulation: the powder addition can be controlled in a large range and the combustion chamber reacts without inertia on different supplies. Moreover, the choice of the sort of coal is by no means restricted.

The definite shape of the most suitable combustion chamber cannot be stated yet from the results of the preliminary tests, but we may take it for granted that coal combustion chambers can be built which, with regard to the performance, can successfully compete with the usual liquid fuel combustion chambers of to-day.

#### B. Coal Vaporization.

The demand of greatest reliability of operation over long working times, as occurring especially with power plants, suggests the idea of burning the coal outside the turbine arrangement and to supply this turbine with a sufficiently cleansed combustible gas if space and construction are not limited. If the temperature of this gas is kept below the melting temperature of slag of the used coal the dust can be removed perfectly from this hot combustible gas through modern means.

Combustible gas is produced according to the method of usual generator arrangements in such a way, that a reduction zone in form of a coal packing is arranged behind the burning zone, to which the described knowledge concerning the design of coal combustion chambers with high loading are applied. In this coal packing the carbon-dioxide-gas arisen in the burning zone is reduced to carbon mon-oxide; thus the gas temperature is decreased to about 1500 °C, provided that the fresh gas enters the generator with an average compressor-end temperature.

By re-cooling the air which is supplied to the generator to the surrounding temperature, the vaporizer-end temperature can be decreased to approximately 1350 °C.

Since this temperature is very near the slag melting point of coal, partly even higher, we are much interested in a more effective cooling for the above-mentioned reasons and in respect of the difficulties implied by the supply of such a hot gas to the combustion chamber. This cooling, however, must not exceed a certain low limit without prejudicing the coal oxide production. The lowest temperature limit, down to which, practically, no coal dioxide remains in the generator gas, with gas pressures of 4 atm (abs) is at about 1000 °C, increasing with 20 atm to about 1100 °C. Below these temperature limits the gas volume first decreases in consequence of the decreasing temperature, but then increases on account of the rapidly increasing CO<sub>2</sub>-proportion. This useless gas causes the dimensions of the generator to become larger than necessary for the production of a certain quantity of combustible gas. If this can be admitted with respect to lower gas temperatures the next limitation results from the reaction velocity decreasing rapidly with falling temperature. This fact causes another enlargement of the vaporization room. Working with temperatures lower than 800 °C, oxygen as another additional gas departs from the generator. In the following considerations, therefore, the decrease in temperature be restricted to 1000 °C.

This decrease can be obtained in known manner by superposing an endothermal process to the described process, i.e. in the vaporizer heat is made chemically bound by a reduction process, and is liberated again in the gas-combustion chamber. Such an endothermal process is initiated by adding CO<sub>2</sub> or H<sub>2</sub>O to the fresh gas entering the vaporizer. The quantity of cooling gas required increases with decreasing vaporizer-end temperature and with increasing vaporizer-entry temperature, which is determined by the end temperatures of the compressor and of the turbine, as well as by the efficiency of the heat exchanger.



# B 1 Coal Vaporization with Addition of CO<sub>2</sub>

When adding CO<sub>2</sub> into the vaporisor almost exactly 1 kg coal dioxide gas is necessary for the vaporization of 1 kg coal to obtain a combustible-gas temperature of 1000° C with an entry temperature of 500° C. The amount of CO<sub>2</sub> needed being considerable, we have to deal with the question whether it can be supplied by means of the exhaust gas. For this purpose, part of the exhaust gas can be cooled in a cooler as approximately as possible to the temperature of the surroundings and can be supplied to the compressor with the fresh air. The quantity of the necessary exhaust gas, among others, depends on the CO<sub>2</sub>-concentration in the exhaust gas which decreases with increasing heating of the compressed fresh air by means of a heat exchanger, and with decreasing turbine-entry temperature. Thus, with a highly efficient heat exchanger and a turbine-entry temperature of 750° C, up to 75 p.c. of the exhaust gas quantity is required. As is seen the greatest part of the working gas is guided in a closed circulation whilst only a smaller part is continuously supplied to the compressor in form of fresh air. The corresponding quantity of exhaust gas is taken from behind the turbine or behind the heat exchanger. The exhaust gas cooler required for this method is very large as the amount of exhaust gas circulating is large and the thermic efficiency required is high, since the temperature of the exhaust gas, owing to its high proportion in the gas flowing through the compressor, governs the compressor and thus its power consumption. A diminution of the cooler as well as of the other elements and engines of the gas turbine plant can be attained by transposing the circular process to a higher level of pressure- as already proposed by S u l z e r regardless of the advantages resulting for the coal vaporization. In this case an additional compressor is needed for supplying fresh air to the circulation, and for removing the exceeding exhaust gases out of the circulation an additional turbine is needed, whose sizes are determined by the fact that they must work up to 30 p.c. of the gas flow on a low pressure level.

The exhaust gas quantity necessary for cooling the combustible gas - leaving the generator - down to 1000° C can be reduced by about one power of ten by increasing the CO<sub>2</sub> - proportion of one of its parts, e.g. in a centrifuge to about

1.5 the value and then supplying it exclusively to the air which enters into the vaporisor. In this case, therefore, a cooler, a centrifuge, and a compressor are additionally needed, whose rate of flow amounts to about 7 p.c. of the gas quantity impinging against the gas turbine.

With regard to the efficiency, these three methods working with CO<sub>2</sub>-cooling do not differ from one another essentially nor from the direct coal combustion. Only the different temperatures resulting slightly alter the radiation losses, the performance of the compressor, etc., which result in little differences which will be taken into account largely by constructive methods.

# B 2 Coal Vaporization with Addition of H<sub>2</sub>O

If the vaporisor is cooled by addition of water we have, however, to deal with different conditions; if we dispose of a sufficient quantity of water, we should always prefer this method.

The smallest quantity of water is required if it is added exclusively to the air supplied to the vaporisor. In this case, we require only approx. 40 per cent of weight of the CO<sub>2</sub> quantity necessary for obtaining an equal cooling. The heat of the exhaust gas suffices for producing this quantity of steam. An increase of the efficiency of this circular process results from the fact that in the turbine there is a higher gas weight than must be worked in the compressor. This fact induces us to examine the question if more fuel can be economised by increased addition of water; this is obtained by adding steam not only to the air led into the vaporisor but also to the whole quantity of air entering the combustion chamber.

The upper limit of the suitable/ addition of water depends on the conditions due to the gas turbine process. The water addition is chiefly limited by the fact that only little use, if any, can be made of the condensation heat for the evaporatio because it happens on a higher pressure level. From this limitation results the necessity of supplying the steam to the circulation process at two places. First so much steam is added, as before, to the air entering the vaporisor, as is necessary for obtaining the desired low temperature of the

combustible gas the remaining steam which can be produced by the exhaust gas is added to the air which enters the combustion chamber immediately.

A third quantity of water, finally can be added to the air already before the entry into the compressor in form of very fine spray. In consequence of the high heat transition figures appearing at these extremely small drops, and on account of the resulting large water surface, this water follows the increasing temperature in the compressor nearly without inertia. The increase in steam pressure connected with this increase in temperature effects an evaporation-cooling of the compressor air and thus a decrease of the compression required. The upper limit of this water quantity is obtained when the air is saturated on leaving the compressor.

The supply of these three quantities of water - the two latter not pre-supposing the vaporization of coal - influences the gas turbine process advantageously for the following reasons. First an approximation to the isothermal alteration of the conditions is obtained with the compression. Then the existence of steam in the air flowing through the vaporiser effects a pulverization of the slag and the demanded decrease of the temperature of the combustible gas. Moreover the gas mixture consumed in the turbine becomes larger than that flowing through the compressor. - Finally the utilization of the exhaust heat will be improved by the use of a heat exchanger since the exhaust gas is cooler when leaving the turbine plant corresponding to the lower compressor-end temperature.

The quantity of water necessary for utilizing these possibilities completely must be a multiple of the weight of coal. One part of this weight can of course be replaced by condensing the water contained in the exhaust gas or when a reduction of the specific performance and of the efficiency is taken into account, by an addition of exhaust gas, according to the cooling by carbon dioxide as mentioned above.

There is, therefore, the possibility of using the same means, which caused a considerable increase of the specific effect and of the efficiency of the gas turbine plant, for making the vaporization efficient. Thus we get a very suitable way of utilizing coal as turbine fuel.

FILE NO.  
B.I.G.S. - 173

COPY NO. 1

15 November 1946

This Interrogation Report contains Information from a German  
Scientist exploited by United Kingdom.

TESTS IN AN ELECTROLYTIC TANK  
ON A RAMMING AND NON-RAMMING  
AIR INTAKE FOR A GAS TURBINE  
POWER PLANT

by

H. HAHNEMANN  
K. BAMMERT

WARNING: Some products and processes described in this report may be the  
subject of U.S. patents. Accordingly, this publication cannot  
be held to give any protection against action for infringement.

JOINT INTELLIGENCE OBJECTIVES AGENCY  
WASHINGTON, D. C.

LIBRARY  
of the  
FOREIGN SYNTHETIC  
LIQUID FUELS DIVISION  
Bureau of Mines

JAN. 1947



Reports and Translations No. 182  
May '46

(M.A.P. VÖLKENRODE) *omit*

... TESTS IN AN ELECTROLYTIC TANK ON A RAMMING AND NON-  
RAMMING AIR INTAKE FOR A GAS TURBINE POWER PLANT

By

H. Hahnemann & K. Bammert

German References:- M - Institute, Mon-list XI, II.  
MAP - Völkenrode - Refs.:- MAP - V 484 - 182 R  
Edited by:- M. Cox

LUFTWAFFE-  
FORSCHUNGSANSTALT  
KARLSRUHE  
KARLSRUHE

Ministry of Aircraft Production, Völkensrode.

April 1946.

Tests in an electrolytic tank on a ramming and non-ramming air  
intake for a gas turbine power plant

by

H. Hahnemann and K. Bammert.

Summary.

The pressure changes in the field of flow round two types of air intake cowling for a gas turbine power plant (Pedden turbine) were investigated under various simulated conditions of air flow in an electrolytic tank. An insight into the points of possible breakaway was gained and a qualitative comparison of the two types of entry was made.

List of Contents.

1. Introduction.
  2. Object of tests and description of types of entry.
  3. Method of tests and results.
    - a) Spinner with ramming intake, without radiator.
    - b) Spinner with ramming intake, with radiator.
    - c) Windtunnel model with modified entry, without radiator.
  4. Closing remarks.
- References.  
List of figures, and letter-press.  
Figures 1 to 28.

Unbefugte Verwendung ist strafbar und strafenspflichtig

Author:	Title:	Series No.	Series Date:	
Editor:	(Date)			

St.-Z. 1. 2. 7. 8. 9. 10. 11. 12. 13. 14. 15. 16. 17. 18. 19. 20. 21. 22. 23. 24. 25. 26. 27. 28.

In an earlier report<sup>1</sup>, a test apparatus was described in which, with a very small amount of effort, the field of flow round plane bodies or bodies of rotation could be easily obtained. The work done to date is described in two reports<sup>1,2</sup>.

The apparatus, an inclined electrolytic tank, makes use of the analogy between the differential equations for potential flow in a fluid and those for the flow of an electric current through an electrolyte, together with other properties of planes of symmetry in the problem to be investigated. As planes of symmetry, across which no streamlines pass, we have on one side an accurate glass plate, upon which the arrangement of any particular problem is built up by boundary walls stuck to the plate; the other plane of symmetry is defined by the free upper surface of the electrolyte with which the tank is filled. With the glass plate lying flat, plane problems are represented; if the glass plate is inclined, then the electrolyte corresponds to a wedge-shaped sector of a rotationally symmetric problem. The boundary walls are usually of a non-conducting material, but if a specific part of them are made electrodes, across which a potential difference is applied, the potential field over the whole surface of the electrolyte may be plotted by means of a moveable electrode dipping onto the surface. This potential field is identical with that of a frictionless field of flow having similar boundary conditions.

Approximate data concerning the apparatus, the best arrangement of the boundary walls, methods of reducing errors and its limitations of use may be studied in the report<sup>1</sup> mentioned above.

The aim of the tests in this tank was to examine the flow round a spinner and air intake cowling of a gas turbine unit in two alternative forms, and to determine the points at which break-away might occur. Fig.1 shows a front view and a cross-section through the part of the unit under consideration. Together, the long spinner 'a' and the intake cowling 'b' form the annular space 'e', through which the air is led to the compressor. The

struts 'c' and 'd' connect the two parts 'a' and 'b'. The annulus 'e' is arranged to utilize the slipstream ram, and dimensioned so that the air is uniformly accelerated. Beneath the unit is an oil cooler 'h' surrounded by a cowling 'g', the air being ducted through a normal type of diffuser 'f', and after leaving the radiator block is mixed with the slipstream tangentially from the nozzle 'i'.

Owing both to the arrangement of the radiator and to the eccentricity of the lower cooling, this is not strictly a rotationally symmetric case. The plane AB through the axis is the only plane of symmetry which will not be intersected by streamlines. In all other planes passing through the axis a normal component of the flow will exist, which, however, can be taken as being small as we approach the symmetrical case. Similarly, the effect of the struts may be neglected.

An ideal shape of the arrangement sketched in fig.1, neglecting these asymmetries, was tested in the tank. Two sectors, BMC and AMC', were chosen, having a wedge angle  $\alpha \approx 10^\circ$ . The first sector corresponds to a rotationally symmetrical case of the part above the horizontal dotted line, the second to the section beneath this line, the radiator being considered to form a complete circular installation. A mean value was chosen for the gap at the entry to the radiator duct.

Fig.2 is a drawing of both sectors altered in this way. AM and BM are bounded by the glass plate, C'M and CM by the free surface of the electrolyte. The extensions of the spinner 'a' and the cowling 'b' and 'c' may be taken as straight lines normal to the glass plate, owing to the angle  $\alpha$  being chosen small; their height is determined by  $\alpha$  and the distance from the axis 'M'). It is obvious that the quantities on the actual turbine unit should lie within the values measured on the two sectors described above.

+) It would be possible approximately to determine the effect of the struts 'c' and 'd' in fig.1 by the construction of further models, on the lines indicated in fig.2b. These refinements would, however, probably be within the limits of sensitivity of the existing type of tank, and it would appear necessary first to make the improvements suggested in reference 1 (i.e. to the electrical circuit and the searching electrode, use of null methods, and a more powerful input signal).

Bezeichnet:	Tag:	Erste Nr.	Erster durch
Prüfer:	Tag:		

Fig. 3 is a cross-section through a model for testing the forward part of the turbine power unit in a wind tunnel. The effect of the compressor is simulated in this model by an electrically driven axial blower situated within the model, which draws in air through the intake 'o'. Similar tests were made on this model, which has a rather faster spinner, in the electrolytic tank. How far the centrifugal force would tend to cause breakaway owing to the sudden changes in direction of the air in the entry duct itself (in spite of the acceleration caused by the deduction in cross-sectional area), leading finally to an undesirable buffeting of the compressor blades, must be left over for a further series of tests. The dimensions of the tank (500 mm x 1100 mm) would only allow an entry of 10 to 20 mm wide to be chosen, if the flow pattern was to be relatively undisturbed by boundary wall effects, so that measurements were not made within the actual entry itself.

### 3. Method of test and results.

#### a) Spinner with entry cowling, without radiator.

Fig. 4 shows the arrangement of the spinner and entry cowling with the special bounding walls fitted onto the glass plate. The dimensions are given in millimeters. The axis of flow, 'e', is defined by a thread stuck to the glass plate 'a'. Having stuck the model to the glass plate, the latter is inclined and filled with the electrolyte, care being taken to ensure that the thread is wetted over its whole length. The contours 'b', 'c' and 'd' were made from compressed laminated wood, covered on the wetted edges with thin sheet of plastic material to avoid swelling.  $E_1$  and  $E_2$  are aluminium electrodes. To obtain the equivalent of a flow into the intake, the potential difference  $V_{12}$  applied across  $E_1$  and  $E_2$  is greater than the potential difference  $V_{13}$  between  $E_1$  and  $E_3$ . In the opposite case, where  $V_{13}$  exceeds  $V_{12}$ , the effect of a resistance to flow through the annular space is simulated. The case  $V_{12} = 0$  and  $V_{13} \neq 0$  represents no flow into the intake. For turbine power plants we are only interested in the case  $V_{12} > V_{13}$ .

So that no important acceleration should occur along the

Unbefugte Verwendung ist strafbar und schadenstiftend

Author	Fig.	Scale	Scale
100	100	100	100

boundary wall streamline 'd', which even in practice is not quite a straight line, the largest cross-section  $R_0$  was chosen to be 160 mm. The boundary wall streamline thus lies at a distance  $3 R_0$  from the axis. In the actual case,  $R_0$  is 396 mm.

Figs 5, 6, 7 and 8 show the potential fields plotted with the above arrangement, using various values of  $V_{12}$  and  $V_{13}$ . The larger of these two voltages may be divided into 110 equal parts by a potentiometer, and the smaller voltage into a correspondingly smaller number of parts of the same size. Only every fifth potential line was plotted completely, the others were plotted for a short distance near the boundaries, the region where the interest lies. For the reasons given above, the lines were only followed a short way into the intake.

The following formula

$$\frac{p - p_0}{q_0} = 1 - \left( \frac{\Delta s_0}{\Delta s} \right)^2 \quad (1)$$

gives the change of pressure along streamlines. The overall voltage was divided into equal potential stages; the more fine these divisions, the more accurately does this formula hold good.  $p$  denotes the static pressure at the point under consideration,  $p_0$  and  $q_0$  the static and total pressures respectively in the free stream, i.e. near electrode  $E_1$ .  $\Delta s_0$  and  $\Delta s$  are the respective distances between adjacent potential lines near  $E_1$  and at the section under consideration. Since the axis of flow and the boundaries of the contours are streamlines, equation (1) may be used to calculate the overall change of pressure. The values calculated from figs. 5 to 8 are shown on figs. 9 to 12. The pressure ratio  $(p - p_0)/q_0$  is plotted against  $x/R_0$ , where  $R_0$  is the radius at the maximum cross-section and  $x$  is the distance from the stagnation point on the spinner, values being taken as positive to the right. All curves are mean lines through the experimental points, which have not been plotted. On each of the four figures curves 'a' show the pressures along the axis in front of the spinner, 'b' along the spinner, 'c' along the outside of the cowling, and 'd' along the boundary wall streamline. The vertical line 'g' indicates the beginning of the intake.

Bearbeiter:

Tag:

Erreicht für

Erreicht durch

Prüfer:

Tag:

Comparison between the figures leads to the following conclusions. From the curves 'a', it is seen that the air is arrested in front of the spinner, the distance in front of the spinner at which this arrest occurs increasing as the resistance to flow into the intake increases. On the other hand when the air is sucked into the intake, the flow clings remarkably closely to the spinner. Along the spinner the pressure falls from the stagnation point onwards, first of all steeply, corresponding to the rapid acceleration, but, with a resistance in the intake, rises again considerably in the region where  $x/R_0 = 1$  to 2, before it receives further acceleration in the intake itself, to the right of 'g' (Curves 'b'). In this case, which, however, does not represent a common practical case, the flow from the entry of the intake cowling must be calculated taking the effect of breakaway into consideration. In the case where the throughput is low, corresponding to no-load conditions on the compressor, there is also a region of pressure rise which indicates local breakaway (fig.11), which finally disappears completely under conditions of powerful suction (fig.12). On the intake cowling there is a further acceleration, curve 'c', and here again the tendency for breakaway to occur decreases with the greater intake to the compressor. Curves 'd' in the first three cases show a small acceleration along the outer boundary wall, so that the true streamlines in the free airstream are a little disturbed. Fig.12, however, under a condition of high airflow into the compressor, shows a practically constant pressure along the boundary wall.

b. Spinner with intake cowling and radiator.

Fig.13 shows the second arrangement, incorporating a radiator to be built into the electrolytic tank. Compared with the arrangement illustrated in fig.4, this has two additional electrodes  $E_4$  and  $E_5$  fitted where the radiator block comes in the actual unit. By means of the electrode  $E_4$ , a potential difference  $V_{14}$ , less than  $V_{13}$ , is applied, simulating a flow into the duct containing a resistance. The continuity of this flow is arranged by electrode  $E_5$ , which maintains the current through, this passage constant. We have, therefore,

$$V_{53} = \frac{w_{53}}{w_{14}} \cdot V_{14} \quad (2)$$

Gezeichnet:	Zeichn. Nr.:	Entworfen von:	Erstellt durch:
Gezeichnet:	Zeichn. Nr.:	Entworfen von:	Erstellt durch:

w being the resistance of the electrolyte between the pairs of electrodes indicated by the suffixes. In the above case,  $w_{53}$  was 8000 ohms and  $w_{14}$  10,000 ohms. At the largest cross-section, the radius  $R_u = 143.5$  mm, and the boundary wall 'e' in this case was placed  $3.3 R_u$  distant from the axis. In the actual unit  $R_u = 356$  mm.

Three cases were treated with this arrangement. Fig. 14 was measured with  $V_{13} = 0.9 \cdot V_{12}$ ,  $V_{14} = 0.7 \cdot V_{12}$  and  $V_{53} = 0.55 \cdot V_{12}$ , and represents a case with a small flow through the radiator block and a relatively small resistance in the block. A case with high flow and a high resistance to flow through the radiator block is illustrated in fig. 15, where  $V_{13} = 0.8 V_{12}$ ,  $V_{14} = 0.5 V_{12}$  and  $V_{53} = 0.4 V_{12}$ . Finally, in Fig. 16,  $V_{13} = 0.8 V_{12}$ ,  $V_{14} = 0$  and  $V_{53} = 0$ , the resistance to flow through the radiator duct is infinity. Figs. 17 to 19 are a plot of values obtained from these three fields by equation (1), pressure ratio  $(p-p_0)/q_0$  being plotted against  $x/R_u$ . As before, curve 'a' shows the pressure along the axis in front of the spinner, and curve 'b' the pressure from the stagnation point up to the region of the intake entry cross-section. The vertical lines  $g_1$ ,  $g_2$  and  $g_3$  show respectively the beginning of the intake cowl, the beginning of the radiator duct, and the end of the radiator duct. Curve 'c<sub>1</sub>' gives the pressure along the entry cowl from its stagnation point up to the entry to the radiator duct, and curve 'c<sub>2</sub>' from the radiator duct exit downstream. The pressure on the outer surface of the radiator duct is shown by curve 'd', and, finally, curve 'e' is the pressure along the boundary wall streamline. Figs. 17 to 19 will be considered in the following conclusions. The arrest in front of the spinner (curves 'a') follows closely the effect obtained in the first arrangement without radiator. Again, curves 'b' show no important differences as between the two arrangements. The influence of the radiator duct is only apparent from the intake entry cross-section rearwards, and causes the small pressure maximum at low air flow to the compressor to become more pronounced at very high resistances to flow through the radiator block. At the front part of the annular cowl it appears unavoidable that there should be a pressure rise, in consequence of its shape and the stagnation effects due

Bearbeiter:  
Führer:

Tag:  
Tag:

Beauftragter:

Erreichte Anzahl:



to the resistance of the radiator (curve 'c<sub>1</sub>'). Clearly it is smallest when the input to the compressor is high and the radiator resistance low, and lowest when the opposite conditions obtain. Possibly the risk of breakaway might be reduced by setting the point of maximum velocity over the air intake cowling rather further rearwards. Downstream of the radiator, the pressure rises again somewhat, since the cooling air was rapidly accelerated in the duct, and the greatest rise occurs with a small resistance in the position of the radiator (curves c<sub>2</sub>). This pressure rise also occurs with zero flow through the radiator duct. On the outer side of the radiator duct, the pressure remains fairly constant (curves d). In every case an acceleration of the flow took place above the electrodes representing the radiator, which could not be explained by us. Whether they may be attributed to the ratios at the duct exit, or whether they were merely caused by some undesired effect of the double electrode, could not be determined. Furthermore the minimum point in this region was rather ill defined. The curves 'e' show similar forms to those in the previous cases.

c. Wind tunnel model with modified entry, without radiator.

The basic differences between the arrangements shown in Figs. 1 and 3 are shown in the cross-section 2, whilst fig. 20 gives the dimensions of the contours used in the tank. The model for the tank was 1.27 times the size of the wind tunnel model. The same potential differences  $V_{12}$  and  $V_{13}$  were used in plotting the potential fields in figs. 21 to 24 as were used to plot figs. 5 to 8. The pressure conditions, calculated from figs. 21 to 24 and plotted on figs. 25 to 28, may be compared directly with those on figs. 9 to 12. It is to be seen that the pressure changes along the boundary wall streamline are to all intents and purposes the same in both cases. The arrest in front of the spinner (curve 'a') appears to be rather less sensitive in the second model to the flow into the intake, no doubt on account of the fatter spinner. A slight local breakaway occurs close to the intake entry, which will probably occur with friction flow and appear in the pressure fall along the length of the spinner when there is a small air flow into the intake. Doing away with the ramming intake also leads to an improvement in the aerodynamic properties, especially at small air intake and air flows.

Author:	Top:	Scale:	Sheet:
Editor:	Rev:		

It is especially clear from figs. 25 to 28 that the acceleration along the intake cowl (curves 'o') is smaller the greater the air flow into the entry; at high air consumptions the pressure even rises a little.

#### 4. Closing remarks.

The tests described above show that, so far as freedom from the chances of breakaway occurring are concerned, the second entry is to be preferred. Since, however, this arrangement does not take advantage of the slipstream ram, the question is raised as to whether the first type should be used in spite of the danger of breakaway. This question will now be examined briefly in terms of a complete power unit installation.

The dynamic pressure  $q = \frac{1}{2} \rho v^2$  ( $\rho$  = density,  $v$  = velocity at the point in question) may be evaluated from the pressure ratio  $(p-p_0)/q_0$  calculated from equation (1)

$$q = q_0 \left( 1 - \frac{p-p_0}{q_0} \right) \quad (3)$$

we have

$$\frac{q_1}{q_2} = \frac{\Delta s_{02}}{\Delta s_{01}} \left[ \frac{1 - \left( \frac{p-p_0}{q_0} \right)_1}{1 - \left( \frac{p-p_0}{q_0} \right)_2} \right] \quad (4)$$

where the suffixes 1 and 2 refer to two geometrically similar arrangements. The values for  $\Delta s_0$  are taken from the plots of the potential fields, and those for  $(p-p_0)/q_0$  from the pressure curves. From figures 9 to 12 and 25 to 28, and the corresponding potential fields, we have, for instance, for the dynamic pressure ratio at the intake entry cross-section,  $q_1/q_2 = 0.49$  with a resistance in the annulus,  $q_1/q_2 = 0.43$  with equal flow outside and inside the cowl,  $q_1/q_2 = 0.53$  with a low air flow into the compressor, and  $q_1/q_2 = 0.72$  with a high air-flow. Suffix 1 refers to the arrangement shown in fig.1, and suffix 2 to fig.3. That these ratios are less than one depends merely on the fact that the second entry is further downstream than the first, and also has a higher velocity over its surface, consequent upon the thicker spinner. The direct comparison of the dynamic head along the contours does not, however, allow definite conclusions to be made on the dynamic head available at the compressor. This depends only on the flight

Unbefugte Verwendung ist strafbar und schadenstiftend

Bearbeiter:	Tag:	Erreichte für:	Erreichte durch:
Prüfer:	Tag:		

speed and altitude, and on the intake frontal area exposed to the slipstream.

The first type allows this ram to be utilised for the acceleration of the flow in the intake duct, and a not inconsiderable pressure rise is attained in front of the compressor entry. At a flight speed of 250 metres per second (560 m.p.h) at an altitude of 5 km (16500 ft.) this is equivalent to adding another stage to the compressor.

In the second type of entry the air must first be drawn into the intake by the compressor, which must also supply the work required to deflect the air into the duct, and to accelerate the air towards the compressor. Furthermore, the compressor has to work at a higher compression ratio and, therefore, more power must be supplied.

If the turbine output is the same for both types, then, at equal exhaust thrusts, the power transmitted to the propeller is greater in the first case than in the second. On the other hand, the tests show <sup>that</sup> the first type will show a greater tendency to breakaway and will, therefore, have a greater drag. Thus, the increased propeller power obtained will be partially counterbalanced and in unfavourable cases may completely outweighed. The latter is possible, if the breakaway in the case of the first cowl causes additional losses over the wings.

To summarise, it may be proposed that the intake should be placed as far forward as possible, and provided with a type of entry designed to use full ram. The best solution which, however, invariably gives certain difficulties in propeller power plants, would be to have an axial entry for the air passing through a hollow spinner, which also permits an aerodynamically favourable cowl, free from tendency to cause breakaway, to be designed.

Translated by: M.Cox.

6th April 1946.

Beaufighter:	Tag:	Spzts für:	Erreichte Anzahl:
Pflicht:	Tag:		

References.

- | No. | Author                                      | Title etc.  |
|-----|---|---|
| 1.  | E. Bokert,<br>H. Hahnemann<br>und L. Ehret. | Über die Aufnahme rotationsymmetrischer<br>Potentialfelder in einem neuartigen<br>elektrolytischen Fögel.<br>Jahrbuch d. deutschen Luftfahrtforschung<br>1944, unpublished.<br>Translated Feb. 1946, Plotting rota-<br>tionally symmetrical potential fields in<br>a new type of electrolytic tank. |
| 2.  | H. Hahnemann<br>und L. Ehret.               | Über den Einfluß starker Schallwellen<br>auf eine stationär brennende Gasflamme.<br>Zeitschr. f. techn. Physik, Bd. 24<br>(1943). S. 228/242.   |

Unbefugte Verwertung ist strafbar und schadenersatzpflichtig

Bearbeiter:	Tag:	Seite Nr.	Gelesen durch:
Prüfer:	Tag:		

Unbefugte Verwendung ist strafbar und schadenersatzpflichtig

- a) Longitudinal section
- b) Front view
- a. Spinner.
- b. Entry cowling.
- c. Struts.
- d. Circumferential bars.
- e. Compressor entry duct.
- f. Radiator entry duct.
- g. Radiator duct cowling.
- h. Radiator block.
- i. Air outlet.
- M. Axis
- $R_o, R_w$ , Maximum radii of cowling
- Angle of wedge-shaped sector
- BMC Sectors chosen
- AMO for tests.

a) Without radiator.	a Spinner.
b) With radiator.	b Entry cowling.
MB, MA Planes of symmetry (Glass plate)	c Radiator cowling.
MQ, MQ' Planes of surface of electrolyte.	d Electrolyte.
	e Searching electrode.
	f Outer wall of the tank.
	g Wedge angle.

a) Longitudinal section.      a Spinner  
b) Front view.                  b Entry cowling.  
c Intake duct to blower.

a Glass plate  $1100 \times 500 \text{ mm}^2$   
b Spinner  
c Entry cowling  
All dimensions in mm.

d Outer wall (boundary stream-  
line)  
e Axis of flow (thread)  
H<sub>1</sub>, E<sub>2</sub>, E<sub>3</sub>, Aluminium elec-  
trodes.

Start date:	Tag:	Block size	Transfer date	
End date:	Tag:			

Fig. 5. Potential field for arrangement shown in fig. 4, with a resistance in the annulus.

- |                       |  |
|-----------------------|--|
| a Spinner             | $E_1, E_2, E_3$ Electrodes.                |
| b Entry cowling       | $V_{12}$ Potential between $E_1$ and $E_2$ |
| c Axis of flow        | $V_{13}$ " " $E_1$ " $E_3$                 |
| d Boundary streamline | $V_{12} = 0.9 V_{13}$                      |

Fig. 6. Potential field for arrangement shown in fig. 4, with equal flow inside and outside cowling.

As for fig. 5, except that:-

$$V_{12} = V_{13}$$

Fig. 7. Potential field for arrangement shown in fig. 4, with low flow into entry.

As for fig. 5, except that:-

$$V_{13} = 0.9 V_{12}$$

Fig. 8. Potential field for arrangement shown in fig. 4, with high flow into entry.

As for fig. 5, except that:-

$$V_{13} = 0.7 V_{12}$$

Fig. 9. Plot of pressure  $(p-p_0)/q_0$  against distance from stagnation point  $x/R_0$ , for fig. 5.

- |                       |                          |
|-----------------------|--------------------------|
| a Along axis          | d Along outer wall       |
| b Along spinner       | e Start of entry cowling |
| c Along entry cowling |                          |

Fig. 10. Plot of pressure  $(p-p_0)/q_0$  against distance from stagnation point  $x/R_0$ , for fig. 6.

As for fig. 9.

Fig. 11. Plot of pressure  $(p-p_0)/q_0$  against distance from stagnation point  $x/R_0$ , for fig. 7.

As for fig. 9.

Bearbeiter:	Tag:	Beurteilt von:	Beurteilt durch:
Prüfer:	Tag:		

Fig. 12. Plot of pressure  $(p-p_0)/q_0$  against distance from stagnation point  $x/R_0$  for fig. 8.

As for fig. 9.

Fig. 13. Arrangement of profiles for spinner and entry with radiator duct.

- |  |  |
|--|--|
| a Glass plate 1100x500 mm <sup>2</sup> | e Outer wall (Boundary streamline)                     |
| b Spinner                              | f Axis for flow (Thread)                               |
| c Entry cowling                        | E <sub>1</sub> to E <sub>5</sub> Electrodes            |
| d Radiator cowling                     | g Insulation between E <sub>4</sub> and E <sub>5</sub> |
- All dimensions in mm  
Dimensions Y<sub>1</sub> and Y<sub>2</sub> are the same as for fig. 4.

Fig. 14. Potential field for arrangement shown in fig. 13, with flow into entry and radiator resistance.

- |                    |  |
|--------------------|--|
| a Spinner          | e Boundary streamline                        |
| b Entry cowling    | f Insulation                                 |
| c Radiator cowling | E <sub>1</sub> to E <sub>5</sub> Electrodes. |
| d Axis of flow     |  |
- $V_{13} = 0.9 V_{12}$ ;  $V_{14} = 0.7 V_{12}$ ;  $V_{53} = 0.55 V_{12}$

Fig. 15. Potential field for arrangement shown in fig. 13, with flow into entry and radiator resistance.

As for fig. 14, except that:-

$$V_{13} = 0.9 V_{12}; V_{14} = 0.5 V_{12}; V_{53} = 0.4 V_{12}$$

Fig. 16. Potential field for arrangement shown in fig. 13, with flow into entry and no flow into radiator.

As for fig. 14, except that:-

$$V_{13} = 0.8 V_{12}; V_{14} = V_{53} = 0.$$

Fig. 17. Plot of pressure  $(p-p_0)/q_0$  against distance from stagnation point  $x/R_0$  for fig. 14.

- |   |  |
|---|--|
| a Along axis                                      | e Along boundary wall                    |
| b Along spinner                                   | g <sub>1</sub> Start of entry cowling    |
| c <sub>1</sub> c <sub>2</sub> Along entry cowling | g <sub>2</sub> Start of radiator cowling |
| d Along radiator cowling                          | g <sub>3</sub> End of radiator cowling   |

Author:	Fig.:	Scale:	Scale:
Date:	Fig.:	Scale:	Scale:

Fig. 18. Plot of pressure  $(p-p_0)/q_0$  against distance from stagnation point  $x/R_0$ , for fig. 15.

As for fig. 17

Fig. 19. Plot of pressure  $(p-p_0)/q_0$  against distance from stagnation point  $x/R_0$ , for fig. 16.

As for fig. 17.

Fig. 20. Arrangement of profiles for model with modified entry.

- a Glass plate  $1100 \times 500 \text{ mm}^2$
  - b Spinner
  - c Entry cowling
  - d Outer wall (boundary streamline)
  - e Axis of flow (thread)
  - $E_1, E_2, E_3$  Aluminium electrodes.
- All dimensions in mm.

Fig. 21. Potential field for arrangement shown in fig. 20, with resistance in the annulus.

- a Spinner
- b Entry cowling
- c Axis of flow.
- d Boundary streamline
- $E_1$  to  $E_3$  Electrodes
- $V_{12} = 0.9 V_{13}$

Fig. 22. Potential field for arrangement shown in fig. 20, with equal flow inside and outside cowling.

As for fig. 21, except that:-

$$V_{12} = V_{13}$$

Fig. 23. Potential field for arrangement shown in fig. 20, with low flow into entry.

As for fig. 21, except that:-

$$V_{13} = 0.9 V_{12}$$

Fig. 24. Potential field for arrangement shown in fig. 20, with high flow into entry.

As for fig. 21, except that:-

$$V_{13} = 0.7 V_{12}$$

Unbefugte Verwendung ist strafbar und schadenstreuerfährlich

Gezeichnet:	Tag:	Gezeichnet:	Tag:
Prüfer:	Tag:		



Fig. 25. Plot of pressure  $(p-p_0)/q_0$  against distance from stagnation point  $x/R_0$ , for fig. 21.

- a Along axis
- b Along spinner
- c Along entry cowling
- d Along boundary wall
- e Start of entry.

Fig. 26. Plot of pressure  $(p-p_0)/q_0$  against distance from stagnation point  $x/R_0$ , for fig. 22.

As for fig. 21.

Fig. 27. Plot of pressure  $(p-p_0)/q_0$  against distance from stagnation point  $x/R_0$ , for fig. 23.

As for fig. 21.

Fig. 28. Plot of pressure  $(p-p_0)/q_0$  against distance from stagnation point  $x/R_0$ , for fig. 24.

As for fig. 21.

Unbefugte Verwendung ist strafbar und schadenersatzpflichtig

Bearbeiter:  
Prüfer:

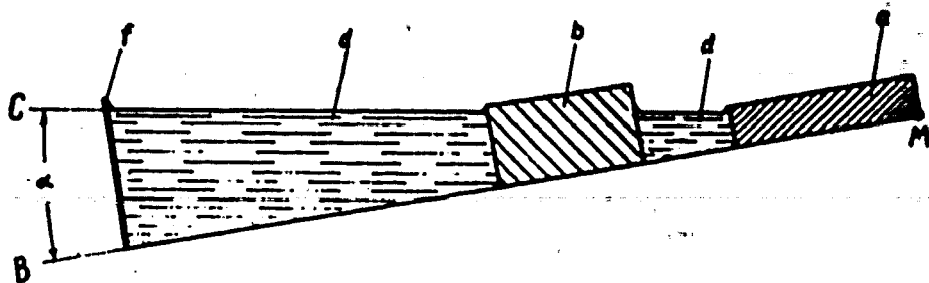
Tag:  
Tag:

Beauftragter:

Beauftragter durch:



a)



b)

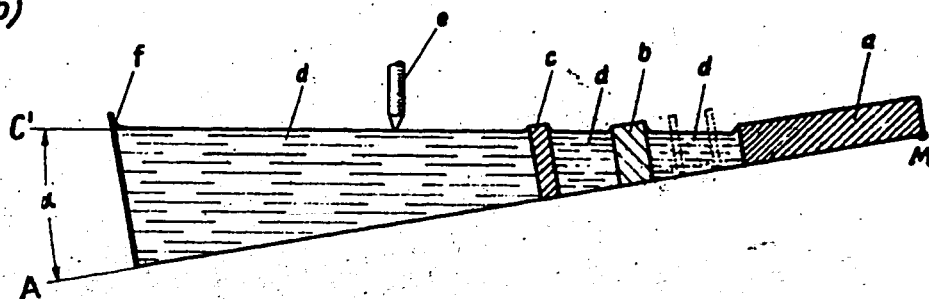


**Bild 2: Schema der Kellanordnung.**

a) ohne Kühler

b) mit Kühler

MB, MA Symmetrieebene (Glasplatte)

MC, MC' Ebene der Elektrolytoberfläche

a) Nabenhaube

b) Einlaufverkleidung

c) Kühlerverkleidung

d) Elektrolyt

e) Spitze der Suchelettrode

f) äußere Begrenzungswand

α Kellwinkel



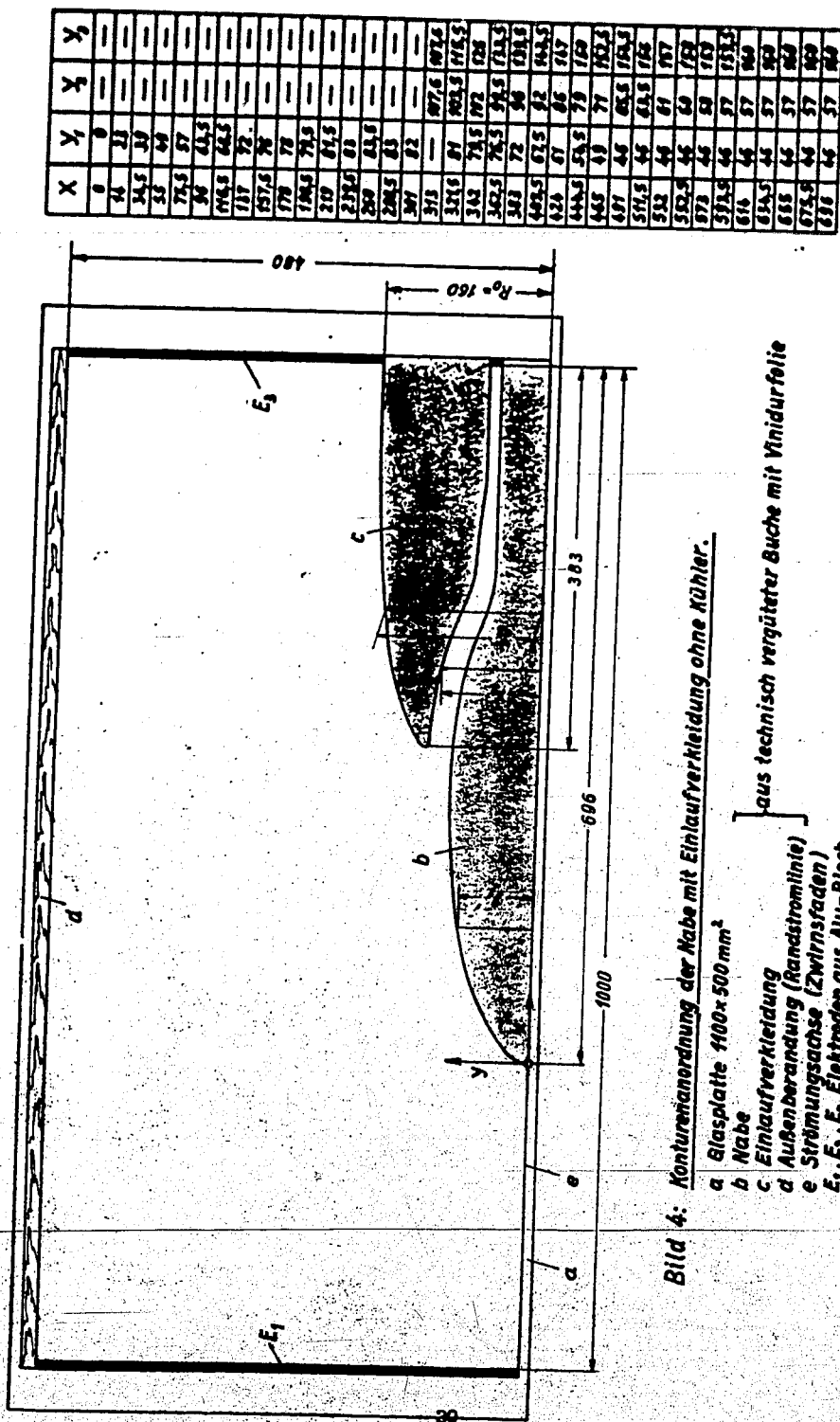


Bild 4: Konturenordnung der Nabe mit Einlaufverkleidung ohne Kühler.

- a Glasplatte 1100x500 mm<sup>2</sup>
  - b Nabe
  - c Einlaufverkleidung
  - d Außenverkleidung (Randstromlinie)
  - e Strömungsschne (Zwischenfaden)
- $E_1, E_2, E_3$  Elektroden aus Alu-Blech  
Abmessungen in mm
- aus technisch vergüteter Buche mit Vinidurfolie

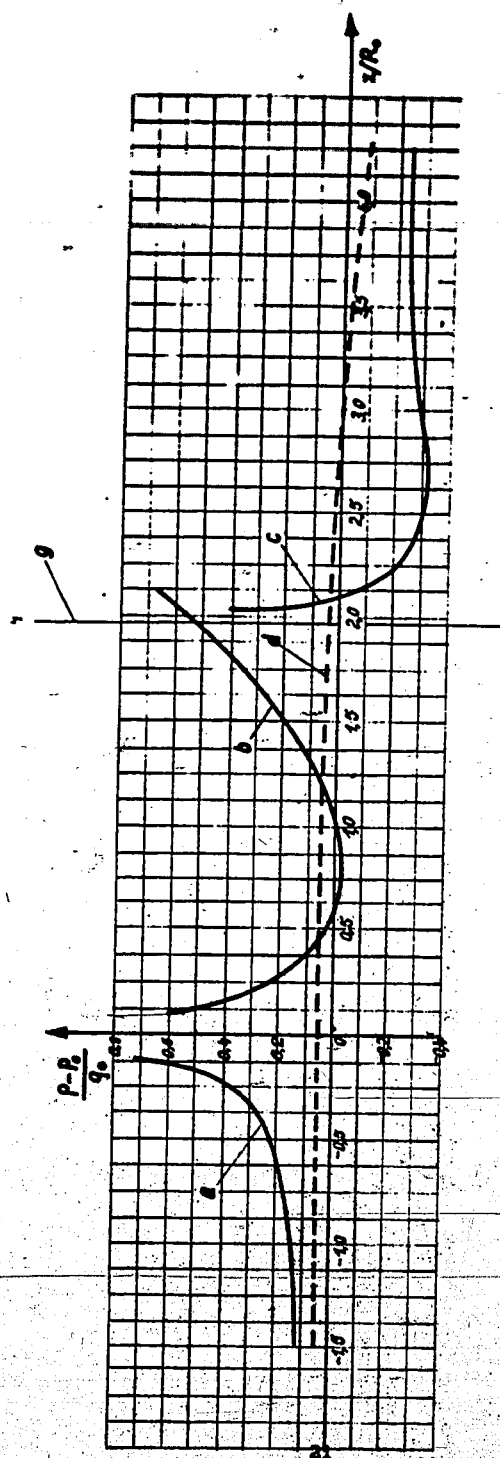


Bild 9: Der Druckverlauf  $\frac{p-p_0}{q_0}$  in Abhängigkeit vom bezogenen Staupunktabstand  $\frac{z}{R_0}$  für die Anordnung nach Bild 5.

- a längs der Achse
- b " " Mitte
- c " " Einlaufverteilung
- d " " Außenverteilung
- g Begrenzung der Verkleidung

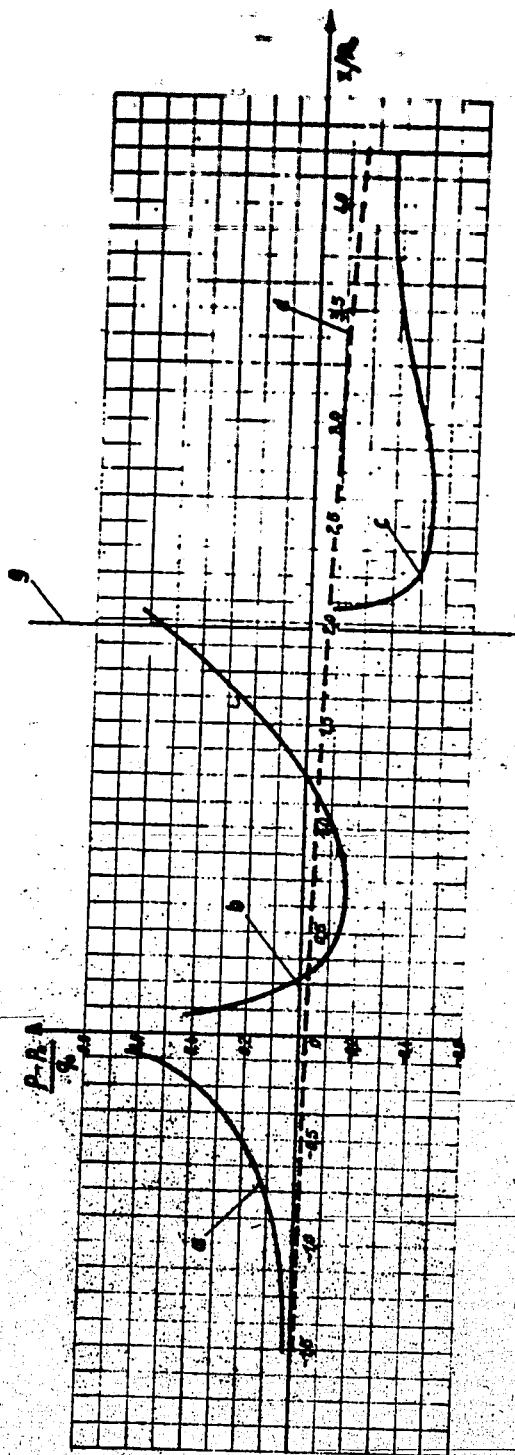


Bild 10: Der Druckverlauf  $p-h$  in Abhängigkeit vom bezogenen Staupunktsabstand  $x/h$  für die Anordnung nach Bild 8.

- a längs der Achse
- b " " Nabe
- c " " Einlaufverteilung
- d " " Außenverteilung
- g Beginn der Verteilung

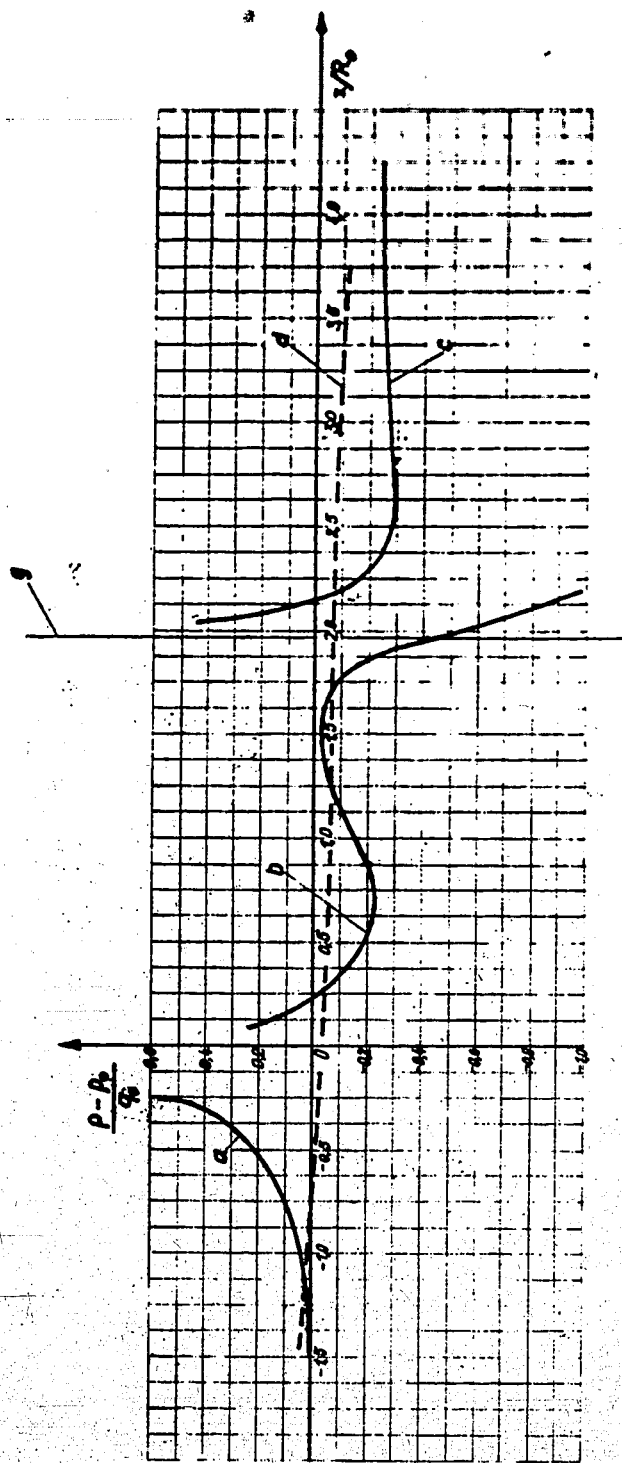


Bild 11: Der Druckverlauf  $\frac{p-p_0}{q}$  in Abhängigkeit vom bezogenen Staupunktsabstand  $x/R_0$  für die Anordnung nach Bild 7.

- a längs der Achse
- b " " " " " " " "
- c " " " " " " " "
- d " " " " " " " "
- g Beginn der Verteilung.



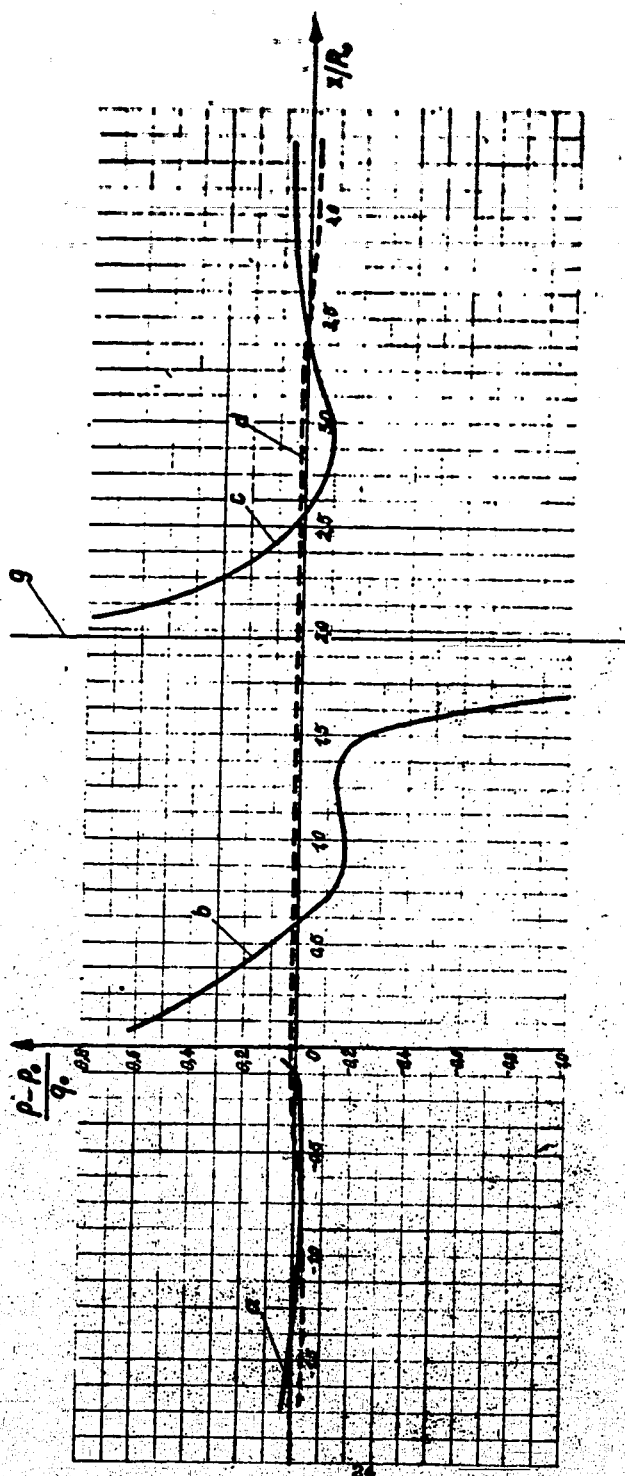


Bild 12: Der Druckverlauf  $\frac{p-p_0}{q_0}$  in Abhängigkeit vom bezogenen Staupunktsabstand  $x/R$  für die Anordnung nach Bild 8.

- a Länge der Achse
- b " " Nahe
- c " " Einlaufverteilung
- d " " Außenverteilung
- g Beginn der Verteilung.

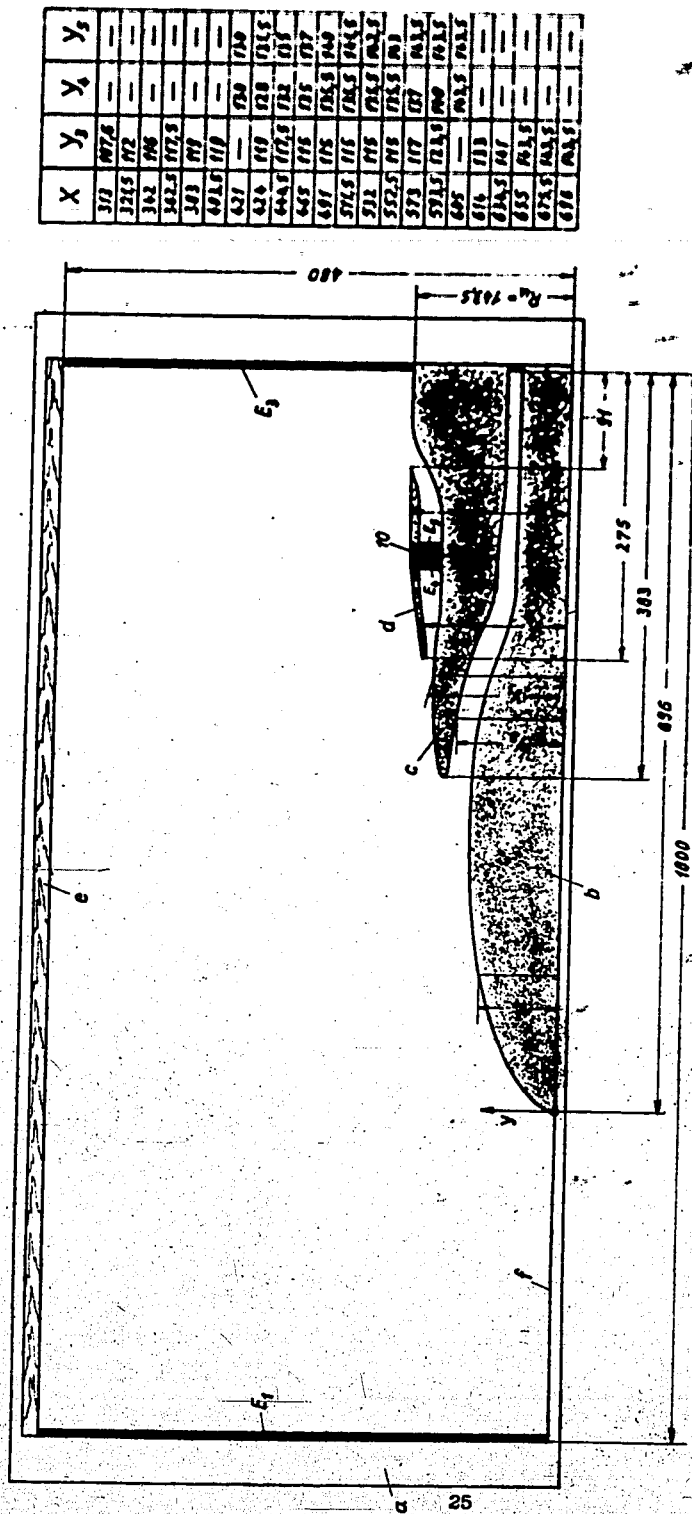


Bild 13: Konturanordnung der Nabe mit Einlaufverkleidung und Kohler.

a Glasplatte 1100 x 500 mm<sup>2</sup>

b Nabe

c Einlaufverkleidung

d Kühlverkleidung

e Außenverkleidung (Randstromlinie)

f Strömungsachse (Zwischenstufen)

E<sub>1</sub>-E<sub>9</sub> Elektroden

g Isolierstück zwischen E<sub>8</sub> und E<sub>9</sub>

Abmessungen in mm

Die Maße für Nabe X<sub>1</sub> und Innenverkleidung Y<sub>2</sub> der Verkleidung sind die gleichen wie in Bild 4.

X	Y <sub>1</sub>	Y <sub>2</sub>	Y <sub>3</sub>
310	877,8	—	—
321,5	772	—	—
342	706	—	—
362,5	772,5	—	—
383	777	—	—
403,5	777	—	—
424	—	730	730
444,5	777	730	730
465	777,5	730	730
485,5	777,5	730	730
506	777,5	730	730
526,5	777,5	730	730
547	777,5	730	730
567,5	777,5	730	730
588	777,5	730	730
608,5	777,5	730	730
629	777,5	730	730
649,5	777,5	730	730
670	777,5	730	730
690,5	777,5	730	730
711	777,5	730	730
731,5	777,5	730	730
752	777,5	730	730
772,5	777,5	730	730
793	777,5	730	730
813,5	777,5	730	730
834	777,5	730	730
854,5	777,5	730	730
875	777,5	730	730
895,5	777,5	730	730
916	777,5	730	730
936,5	777,5	730	730
957	777,5	730	730
977,5	777,5	730	730
998	777,5	730	730

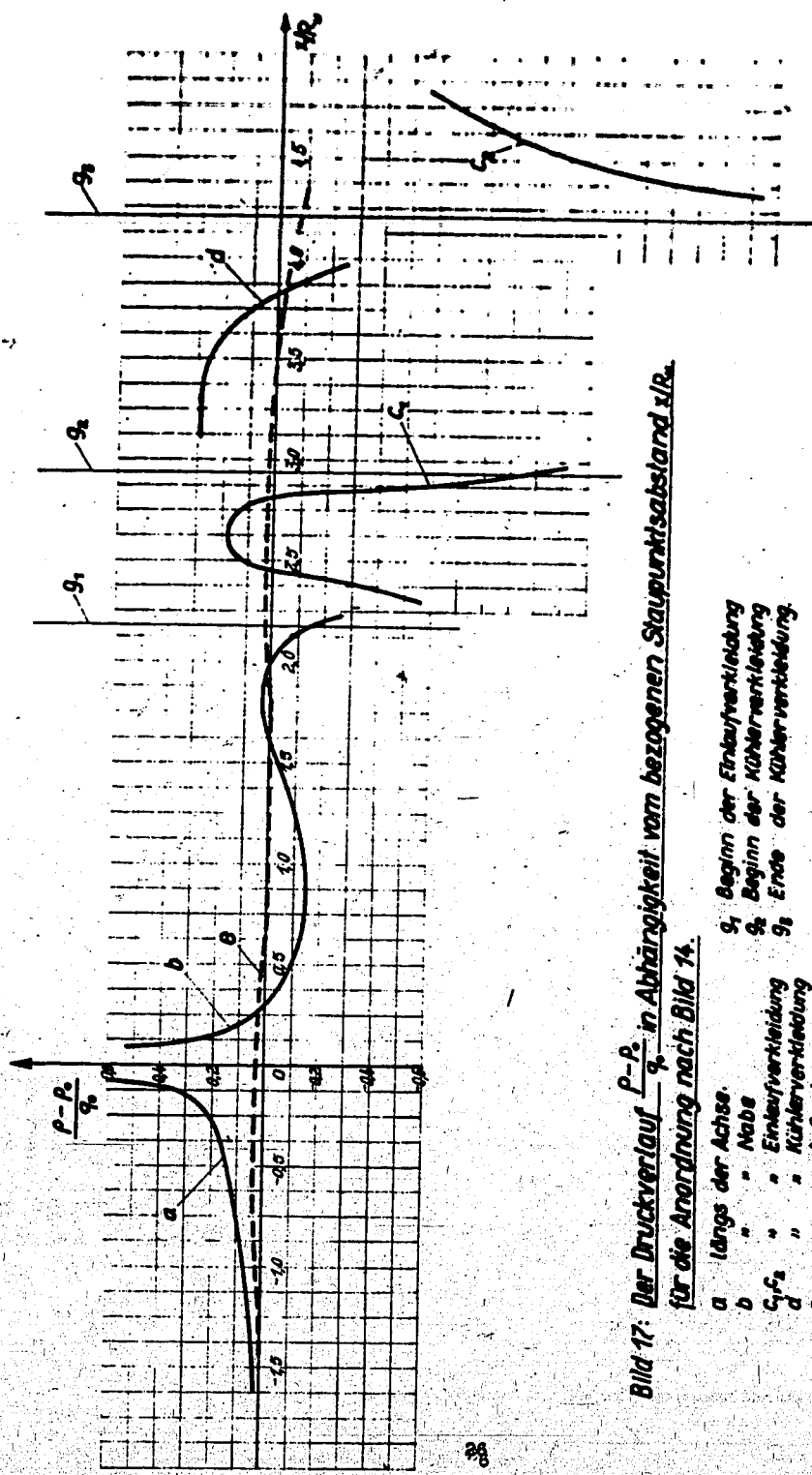


Bild 17: Der Druckverlauf  $\frac{p - p_0}{q_0}$  in Abhängigkeit vom bezogenen Staupunktsabstand  $x/R_0$  für die Anordnung nach Bild 14.

- |                                 |                        |                |                               |
|---------------------------------|------------------------|----------------|-------------------------------|
| a                               | längs der Achse.       | g <sub>1</sub> | Beginn der Einlaufverkleidung |
| b                               | " " Nabe               | g <sub>2</sub> | Beginn der Kühlerverkleidung  |
| c <sub>1</sub> , c <sub>2</sub> | " " Einlaufverkleidung | g <sub>3</sub> | Ende der Kühlerverkleidung    |
| d                               | " " Kühlerverkleidung  |                |                               |
| e                               | " " Außenverkleidung   |                |                               |

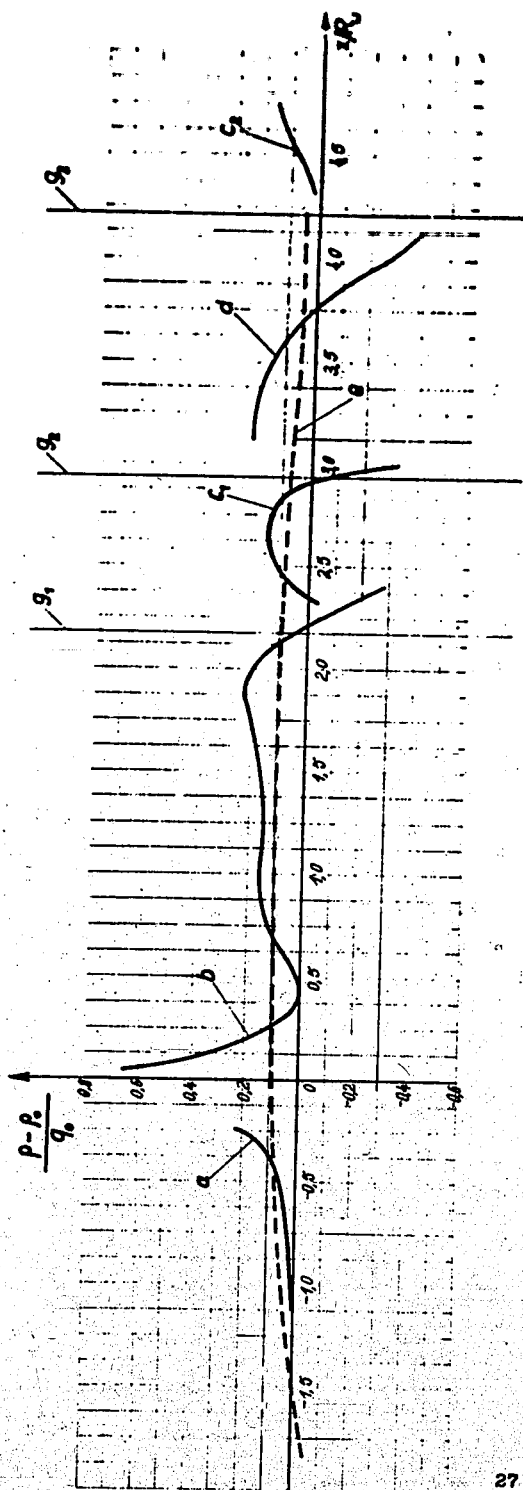


Bild 18: Der Druckverlauf  $\frac{P-P_s}{q_0}$  in Abhängigkeit vom bezogenen Staupunktsabstand  $x/R_0$  für die Anordnung nach Bild 15.

- |              |                      |       |                               |
|--------------|----------------------|-------|-------------------------------|
| a            | längs der Achse      | $g_1$ | Beginn der Einlaufverkleidung |
| b            | " Nabe               | $g_2$ | Beginn der Kühlerverkleidung  |
| c, $\zeta_1$ | " Einlaufverkleidung | $g_3$ | Ende der Kühlerverkleidung    |
| d            | " Kühlerverkleidung  |       |                               |
| e            | " Außenberandung     |       |                               |

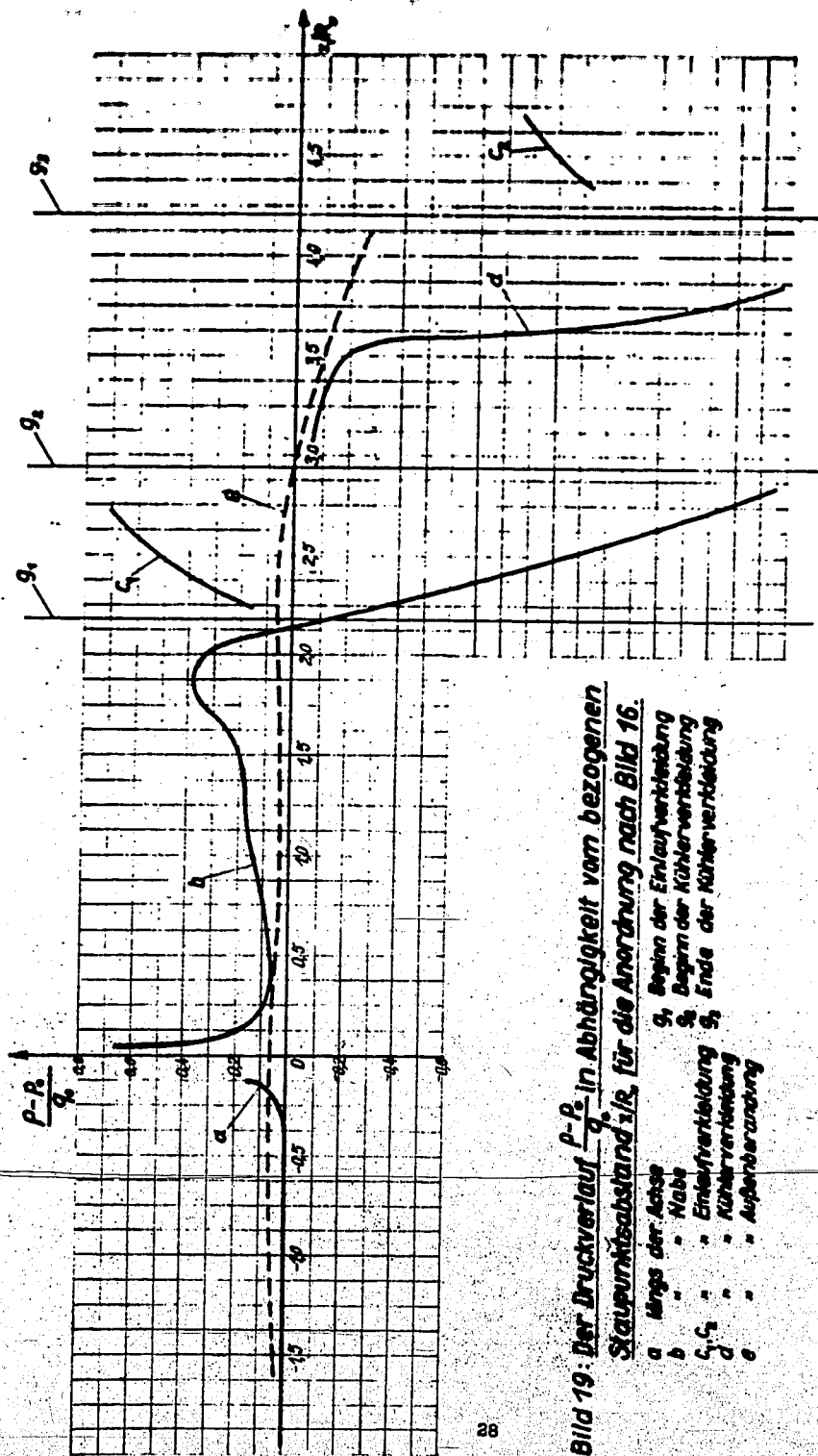


Bild 19: Der Druckverlauf  $\frac{P-P_2}{q}$  in Abhängigkeit vom bezogenen Staupunktsabstand  $s/s_2$  für die Anordnung nach Bild 16.

- |                                 |                              |
|---------------------------------|------------------------------|
| a                               | Beginn der Einlaufverteilung |
| b                               | Beginn der Kühlerverteilung  |
| c <sub>1</sub> , c <sub>2</sub> | Ende der Einlaufverteilung   |
| d                               | Ende der Kühlerverteilung    |
| e                               | Außenverteilung              |



**a. Glasplatte 1100 x 500 mm<sup>2</sup>**

- b** Nabe  
**c** Einlaufverleumdung  
**d** Außenverleumdung (Handstromlinie)  
**e** Strömungsachse (Zwinstromlin)  
**f**  $E_1, E_2, E_3$  Elektroden aus Alu-Blech  
Abmessungen in mm

**aus technisch vergüteter Buche mit Windurfolle**

X	K	K	K	K
0	—	—	—	—
1	—	—	—	—
2	—	—	—	—
3	—	—	—	—
4	—	—	—	—
5	—	—	—	—
6	—	—	—	—
7	—	—	—	—
8	—	—	—	—
9	—	—	—	—
10	—	—	—	—
11	—	—	—	—
12	—	—	—	—
13	—	—	—	—
14	—	—	—	—
15	—	—	—	—
16	—	—	—	—
17	—	—	—	—
18	—	—	—	—
19	—	—	—	—
20	—	—	—	—
21	—	—	—	—
22	—	—	—	—
23	—	—	—	—
24	—	—	—	—
25	—	—	—	—
26	—	—	—	—
27	—	—	—	—
28	—	—	—	—
29	—	—	—	—
30	—	—	—	—
31	—	—	—	—
32	—	—	—	—
33	—	—	—	—
34	—	—	—	—
35	—	—	—	—
36	—	—	—	—
37	—	—	—	—
38	—	—	—	—
39	—	—	—	—
40	—	—	—	—
41	—	—	—	—
42	—	—	—	—
43	—	—	—	—
44	—	—	—	—
45	—	—	—	—
46	—	—	—	—
47	—	—	—	—
48	—	—	—	—
49	—	—	—	—
50	—	—	—	—
51	—	—	—	—
52	—	—	—	—
53	—	—	—	—
54	—	—	—	—
55	—	—	—	—
56	—	—	—	—
57	—	—	—	—
58	—	—	—	—
59	—	—	—	—
60	—	—	—	—
61	—	—	—	—
62	—	—	—	—
63	—	—	—	—
64	—	—	—	—
65	—	—	—	—
66	—	—	—	—
67	—	—	—	—
68	—	—	—	—
69	—	—	—	—
70	—	—	—	—
71	—	—	—	—
72	—	—	—	—
73	—	—	—	—
74	—	—	—	—
75	—	—	—	—
76	—	—	—	—
77	—	—	—	—
78	—	—	—	—
79	—	—	—	—
80	—	—	—	—
81	—	—	—	—
82	—	—	—	—
83	—	—	—	—
84	—	—	—	—
85	—	—	—	—
86	—	—	—	—
87	—	—	—	—
88	—	—	—	—
89	—	—	—	—
90	—	—	—	—
91	—	—	—	—
92	—	—	—	—
93	—	—	—	—
94	—	—	—	—
95	—	—	—	—
96	—	—	—	—
97	—	—	—	—
98	—	—	—	—
99	—	—	—	—
100	—	—	—	—

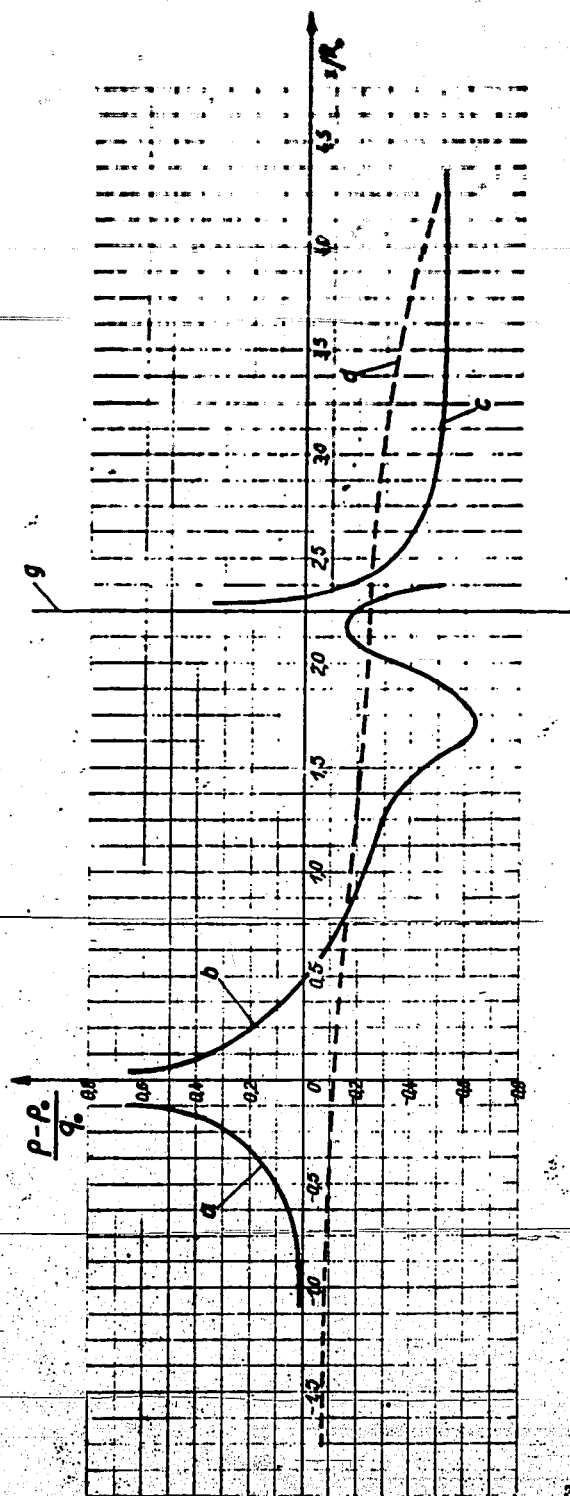


Bild 26: Der Druckverlauf  $\frac{p-p_0}{q_0}$  in Abhängigkeit vom bezogenen Staupunktsabstand  $x/R$  für die Anordnung nach Bild 22.

- a längs der Achse
- b . . . . . Naabe
- c . . . . . Einlaufverkleidung
- d . . . . . Außenberandung
- g Beginn der Verkleidung

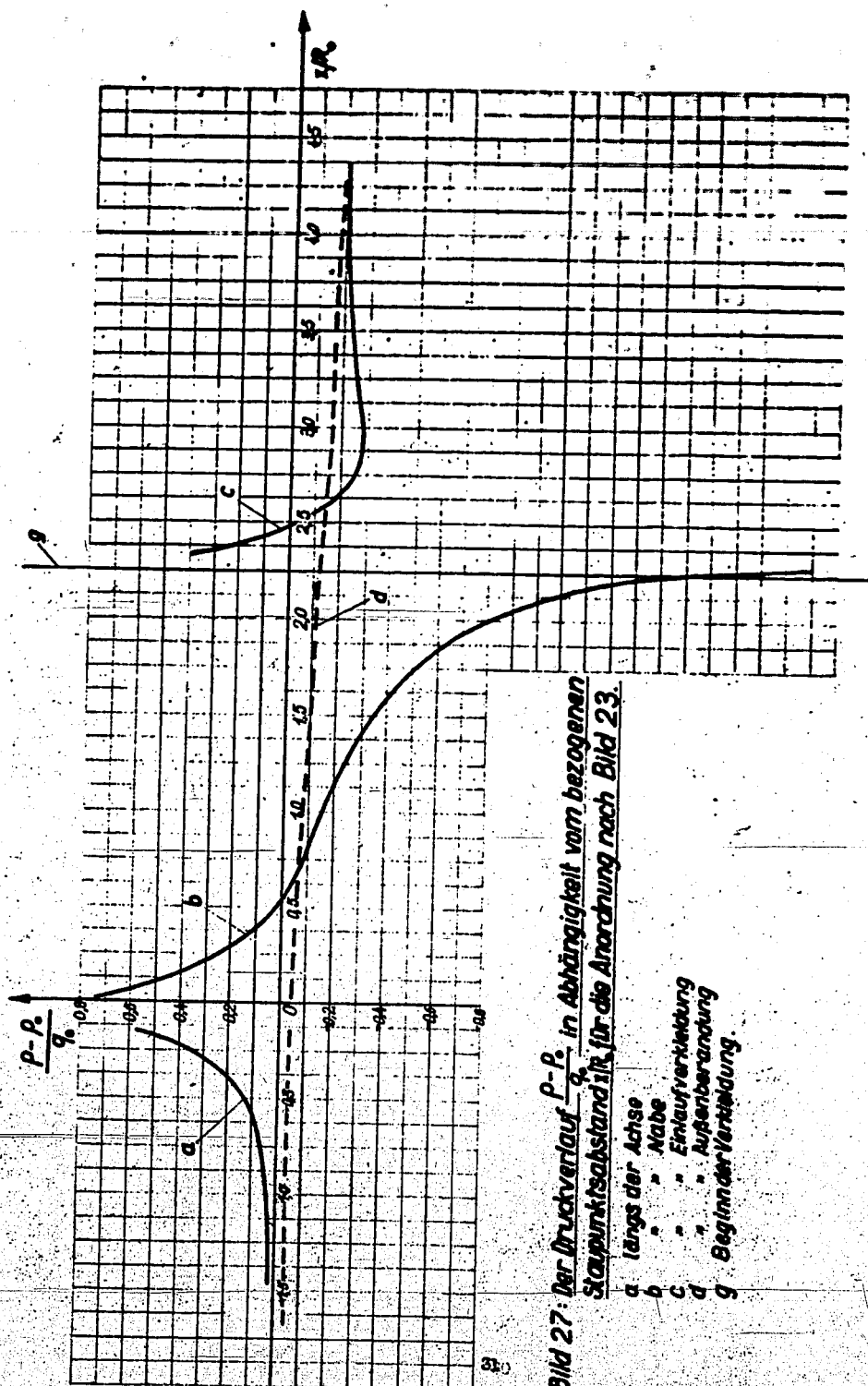


Bild 27: Der Druckverlauf  $\frac{p-p_0}{q_0}$  in Abhängigkeit vom bezogenen Staupunktsabstand  $\frac{x}{R_0}$  für die Anordnung nach Bild 23.

- a längs der Achse
- b " " Nahe
- c " " Einlaufverklebung
- d " " Außenberandung
- e Beginn der Verklebung



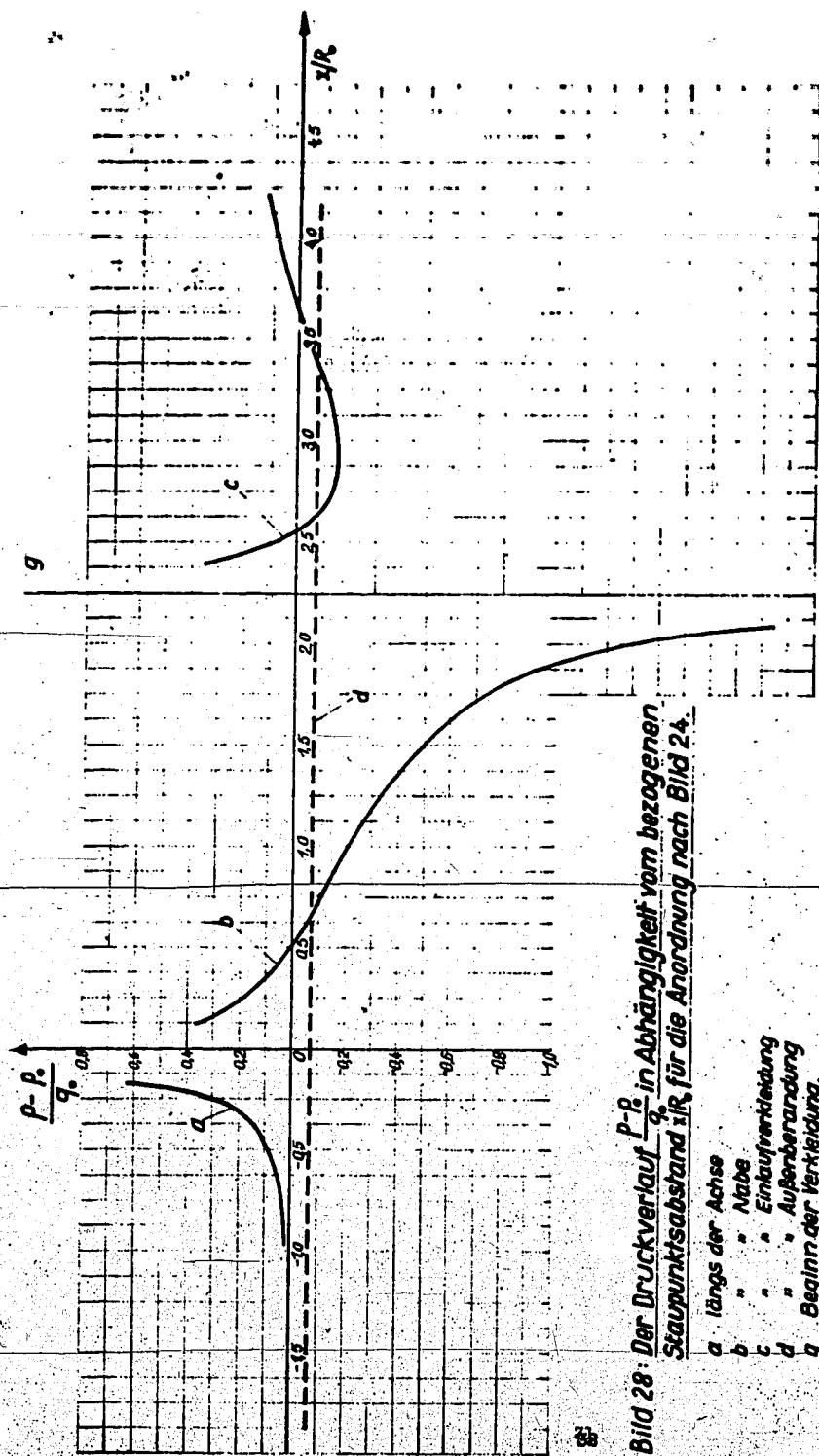


Bild 28: Der Druckverlauf  $\frac{p-p_0}{q_0}$  in Abhängigkeit vom bezogenen Staupunktsabstand  $x/R$  für die Anordnung nach Bild 24.

- a : längs der Achse
- b : " " Nabe
- c : " " Einlaufverkleidung
- d : " " Außenverkleidung
- g : Beginn der Verkleidung.

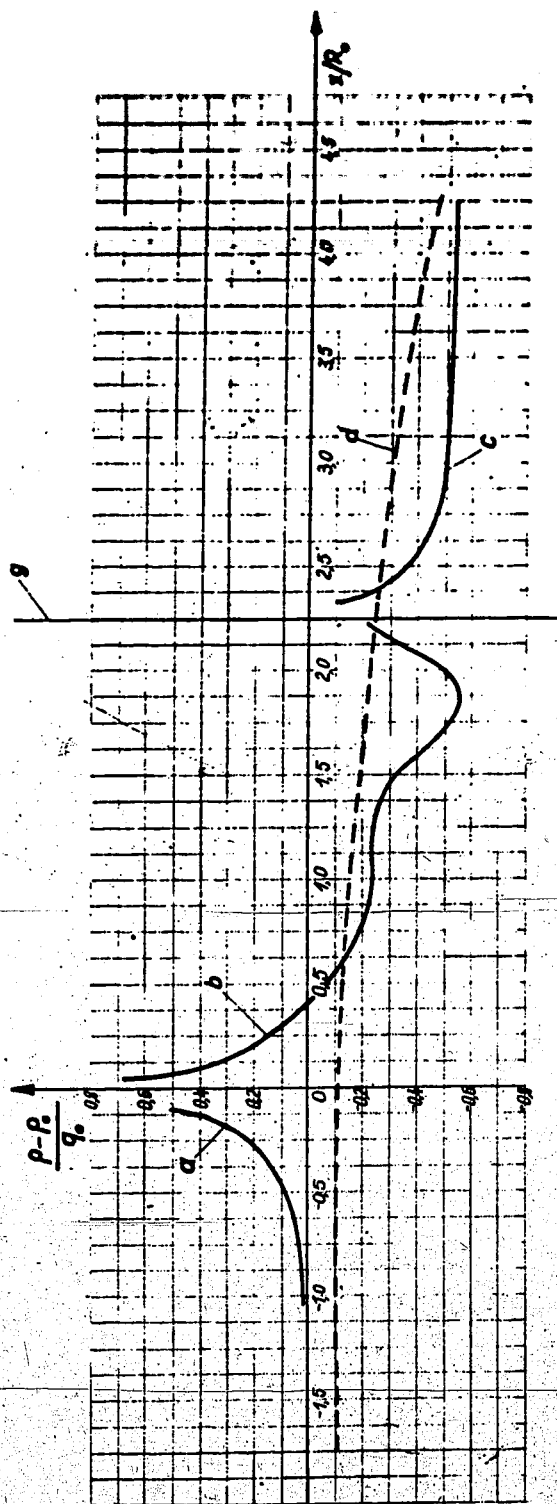


Bild 25: Der Druckverlauf  $\frac{p-p_0}{q_0}$  in Abhängigkeit vom bezogenen Staupunktabstand  $x/R$  für die Anordnung nach Bild 21.

- a längs der Achse
- b " " " " " " "
- c " " " " " " "
- d " " " " " " "
- e " " " " " " "
- f " " " " " " "
- g Beginn der Verteilung

**END**

**T.O.M. REEL**

**B.M. 26**

**D**

**EL 140**

**26**